Cleared: October 25th, 1972
Clearing Authority: Air Force Flight Dynamics Laboratory

DESIGN, FABRICATION, TESTING, AND DATA ANALYSIS OF ADAM II CONCEPT (PROPULSIVE WING)

PART II, SHAKEDOWN TESTING IN VAD 7-FT X 10-FT LOW SPEED WIND TUNNEL

Robert D. Meyer
Robert B. English
Jim K. Davidson

FOREWORD

The work reported upon herein was performed by the Vought Aeronautics Division (VAD) of the LTV Aerospace Corporation of Dallas, Texas, under Contract Nr. AF33(615)-3293, Project Nr. 1366, Task Nr. 136617, supported jointly by the United States Air Force and the United States Army. Air Force support for this effort was made possible through the use of Air Force Flight Dynamics Laboratory Director's Funds. After shakedown testing by the Contractor, the major tests were conducted by the NASA Langley Research Center, Hampton, Virginia, in the 17-foot test section of the LRC 7-foot x 10-foot wind tunnel and in the LRC 16-foot transonic wind tunnel.

The actual wind tunnel testing was started on 2 December 1966 and was completed on 7 July 1967. This report was submitted by the authors in December, 1967.

Acknowledgements are due to many individuals in the Air Force, the Army, and the Langley Research Center. Particular reference is made to Mr. P. P. Antonatos of the Air Force Flight Dynamics Laboratory, who suggested the use of a single model for high and low speed testing in the Langley Research Center wind tunnels; to Messrs. F. M. Rogallo, R. E. Kuhn, A. D. Hammond, K.E. Spreeman, and Garl C. Gentry of the LRC Low Speed Vehicle Branch, who conducted the low speed testing; to Messrs. B. W. Corson, Jr., J. F. Runckel, J. Schmeer, L. B. Salters, Jr., E. M. Brummal, C. F. Whitcomb, and E. E. Lee, Jr., of the LRC 16-foot Transonic Wind Tunnels Branch, who conducted the high speed testing; and to Messrs. J. Gaurino and Carl Roberts of the LRC Instrumentation Research Department, and Mr. John Wilson of the Air Force Flight Dynamics Laboratory, who assisted in resolving problems in the internal strain gage balance used for high speed testing.

The use of photographs of the model in the Langley Research Center Wind Tunnels, furnished by LRC, is gratefully acknowledged.

The program monitor for the Air Force was Major Edward P. Miller, FDMM, Air Force Flight Dynamics Laboratory, Wright-Patterson Air Force Base, Ohio, assisted by Mr. Robert R. Jeffries of the same organization. The program monitor for the Army was Mr. LeRoy T. Burrows, SAVFE-TP, U. S. Army Aviation Materiel Laboratories, Fort Eustis, Virginia. The principal investigator for the Contractor was Mr. B. R. Winborn.

This report is presented in four parts as follows:

Design, Fabrication Testing, and Data Analysis of ADAM II Concept (Propulsive Wing), Part I General and Summary Information

Design, Fabrication Testing, and Data Analysis of ADAM II Concept (Propulsive Wing), Part II Shakedown Testing in the VAD 7-foot by 10-foot Low Speed Wind Tunnel

Design, Fabrication Testing, and Data Analysis of ADAM II Concept (Propulsive Wing), Part III Hover and Transition Mode Testing in the 17-foot Test Section of the Langley Research Center 7-foot by 10-foot Low Speed Wind Tunnel

Design, Fabrication Testing, and Data Analysis of ADAM II Concept (Propulsive Wing), Part IV Cruise Mode and High Speed Testing in the Langley Research Center 16-foot Transonic Wind Tunnel

This technical report has been reviewed and is approved.

Philip P. Antonatos
PHILIP P. ANTONATOS
Chief, Flight Mechanics Division
Air Force Flight Dynamics Laboratory

ABSTRACT

An analysis is presented of the data obtained from a short series of tests to "shakedown" a powered model of the ADAM II V/STOL concept. Correlating data from tests of a related semispan model are also included. Results show that the longitudinal stability of the present configuration in the cruise mode has a greater variation with angle of attack and power than conventional airplanes. The data indicated that, for this test, possible lower surface flap separation and detached nose fan exit flow caused nonlinearities in pitching moment. These can be eliminated by redesign at critical points to provide good stability. The location of the horizontal tails in the wing tip vortex results in an upwash derivative (negative $d\epsilon/d\alpha$) that results in a high level of horizontal tail contribution to stability. Although the basic low aspect ratio horizontal tails were highly loaded and operating with disturbed flow conditions much of the time, there was no indication of tail stall. Horizontal tail control effectiveness appears to be adequate at the present stability levels. The model was less stable directionally than longitudinally in the sense that a greater forward movement in c.g. location is required for neutral stability. In this test, directional stability was independent of angle of attack and power effects, and lateral stability was at all times positive and varied with angle of attack and power effects.

TABLE OF CONTENTS

LIST OF ILLUSTRATIONS

SECTION I

INTRODUCTION

This report concerns the results of LTV low speed wind tunnel test 299 to check out the power system, remote actuators, and model fit prior to entry in the NASA tunnels. The test was primarily of the cruise mode with zero vane box and flap deflections. A run log of the test is presented in the appendix. The results are compared with those of a semispan model of similar configuration. The essential differences between this model and the related semispan model (of LTV LSWT test 172) are shown in Figure 1, these differences being the wing cross section and airflow provisions, nose fan, and horizontal tails. Both low and high aspect-ratio horizontal tails were tested on the full-span model. No tuft photographs or pressure data were obtained from the shakedown test. Tuft observations were recorded, however, and are used in the analysis. Irregularities in lift and moment curves have at times been refaired where it appeared the true stability picture would be in better focus. The refaired curves are shown as dashed lines together with the actual data presented in the figures.

All of the data presented include thrust in the force and moment coefficients. The level of thrust is indicated by net thrust coefficient. Momentum coefficient based on wing fan plus primary gross thrust is used for comparison with previous test results. Momentum coefficient (or gross thrust coefficient), defined by $C_\mu = \Sigma F_G/qS$, is the accepted correlating parameter for jet flap work and was adopted for the ADAM propulsive wing. For the special case of the jet flap, $C_\mu = \dot{m}_J V_J/qS$. For this model, $C_\mu = \Sigma\left|(\dot{m}_f + \dot{m}_c)V_J/g\right|/qS$, since the compressed air used to drive the tip turbine fans and simulate the primary flow is added to the system. The momentum coefficients in this report do not include the nose fan and its drive air gross thrust. Net thrust is gross thrust less ram drag; therefore, the net thrust coefficient for the model is: $C_T = \Sigma\left|(\dot{m}_f + \dot{m}_c)V_J/g - \dot{m}_f V_o/g\right|/qS$. The net thrust coefficients in this report include nose fan gross thrust, drive air, and ram drag. An additional ram drag corresponding to the compressed air mass flow, $W_a V_o/g$, would be present on the airplane. For ADAM II tests, gross thrust and subsequently momentum coefficient was computed from pressure distributions at the primary, secondary, and nose fan flow exits. The distribution of gross thrust among the propulsive flows on the model was, in general, approximately 17% for each of the five fans, and 7.5% for each of the left- and right-wing primary exists. VAD has done some private development of thrust removal techniques. However, additional work is required before the external aerodynamic forces can be separated. Since the measured aerodynamic coefficients include thrust, large lift coefficients, large pitching moment coefficients and large negative drag coefficients are to be expected.

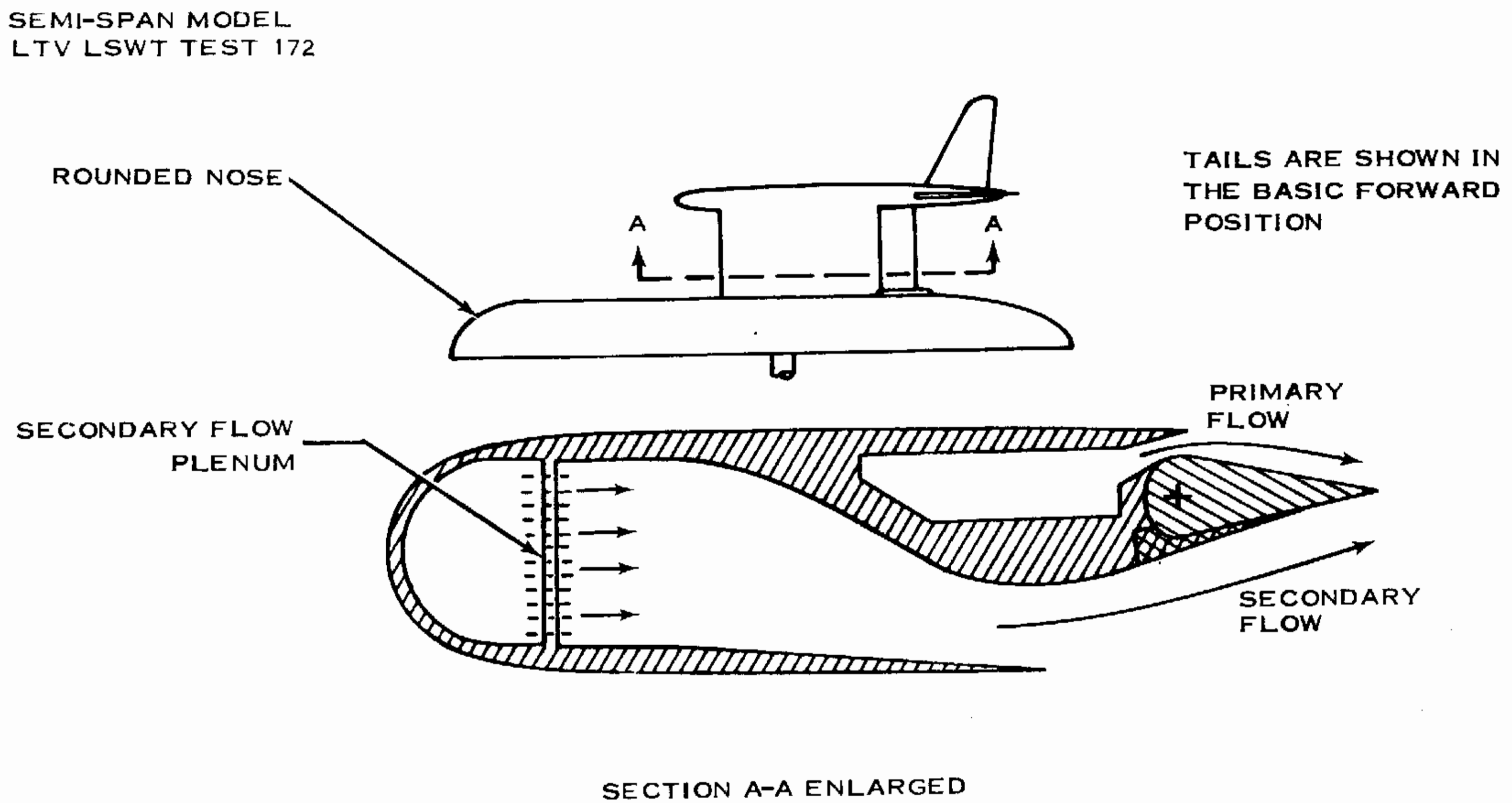

(a) SEMI-SPAN MODEL

Figure 1. Semi-Span and Full-Span Model Comparison

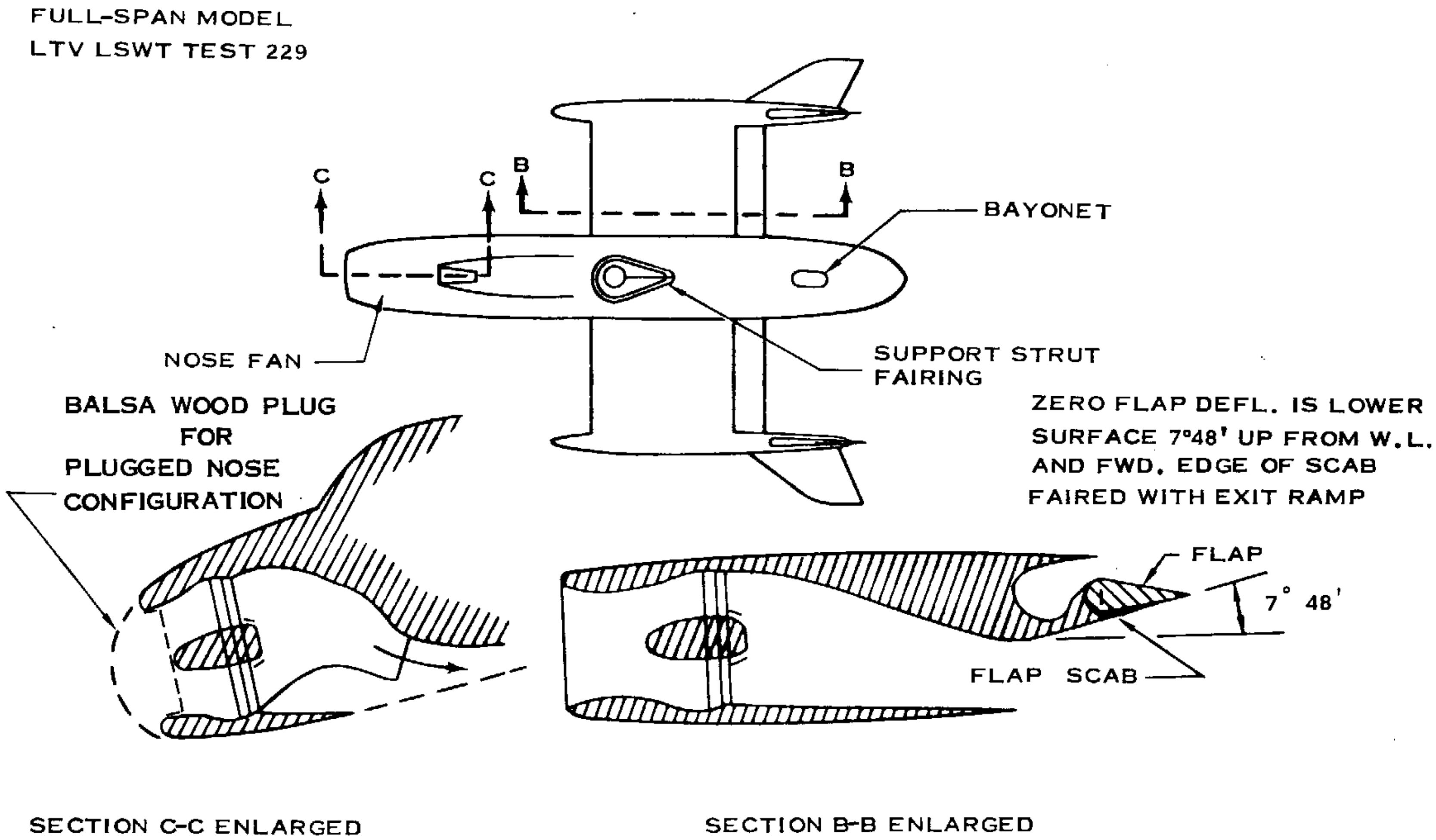

(b) FULL-SPAN MODEL

Figure 1. Semi-Span and Full-Span Model Comparison (Concluded)

It was found that the inclusion of thrust in the data did not particularly detract from the analysis. Since the definition of C_μ has free stream dynamic pressure in the denominator, the actual airplane operating range of C_μ extends from about 0.03 at high speed flight to infinity at hover.

SECTION II

LONGITUDINAL STABILITY

There are three regions in the ADAM II pitching moment data where different types of flow conditions seem to apply, as shown in Figure 2. Region 1 is where the model functions in a normal, linear fashion. In region 2, an unstable change in slope occurs which is believed to be caused by flow separation from the flap lower surface, aft fuselage, or booms. In region 3, a stable change in slope occurs, believed to be caused by a reduction in the destabilizing contribution of the nose fan, the mechanics of which are not certain. A further increase in angle of attack results in a decrease in stability for low values of wing C_μ, $\left(\frac{\text{gross thrust}}{qS}\right)$, due to suspected flow separation from the flap upper surface at an angle of attack of 15 degrees (Figure 3, runs 19 and 28). At the higher values of C_μ, upper surface wing stall occurs at an angle of attack of 30 degrees where the flap upper surface is maintained unstalled due to BLC effect of the primary flow.

These conclusions are based on the tail-off and tail-on lift and pitching moment curves presented in Figure 3. The short dashed line is an arbitrary fairing where thrust is inconsistent. Momentum and net thrust coefficients quoted in this report are average values during a run. The long dashed lines are drawn to make the slope changes of regions 2 and 3 more evident. Data were taken with and without the flap "scab" shown in Figure 1(b). With the scabs off, the flap deflection for runs 11 and 12 was 20° T.E. up to obtain alignment of the lower flap surface. The three stability "regions" are evident in the pitching moment curves, particularly at low values of C_μ.

In moving downward from region 1 to region 2, the fact that the slope changes at $\alpha = 0$ indicates that a flow condition change is caused by some type of model asymmetry. From Figure 1(b) this would be either the nose fan with the under fuselage exit, or the area including the wing box, flap and jet flow exits. In considering low values of C_μ where the effect is most apparent (runs 19 and 28), the reduction in lift curve slope in region 2 with an unstable shift in the moment curves suggests a stalled region behind the moment reference point. The lower surface of the flap is suspect because at negative angles of attack, there is an expansion of the secondary fan flow required between the flap lower surface and the streamline from the lower wing trailing edge. This expansion produces an adverse pressure gradient along the lower flap surface and a tendency for the flow to separate from the lower flap surface. A comparison of the tail-off moment curves for the windmilling case, C_μ = "0," with and without flap scabs (flap 20°

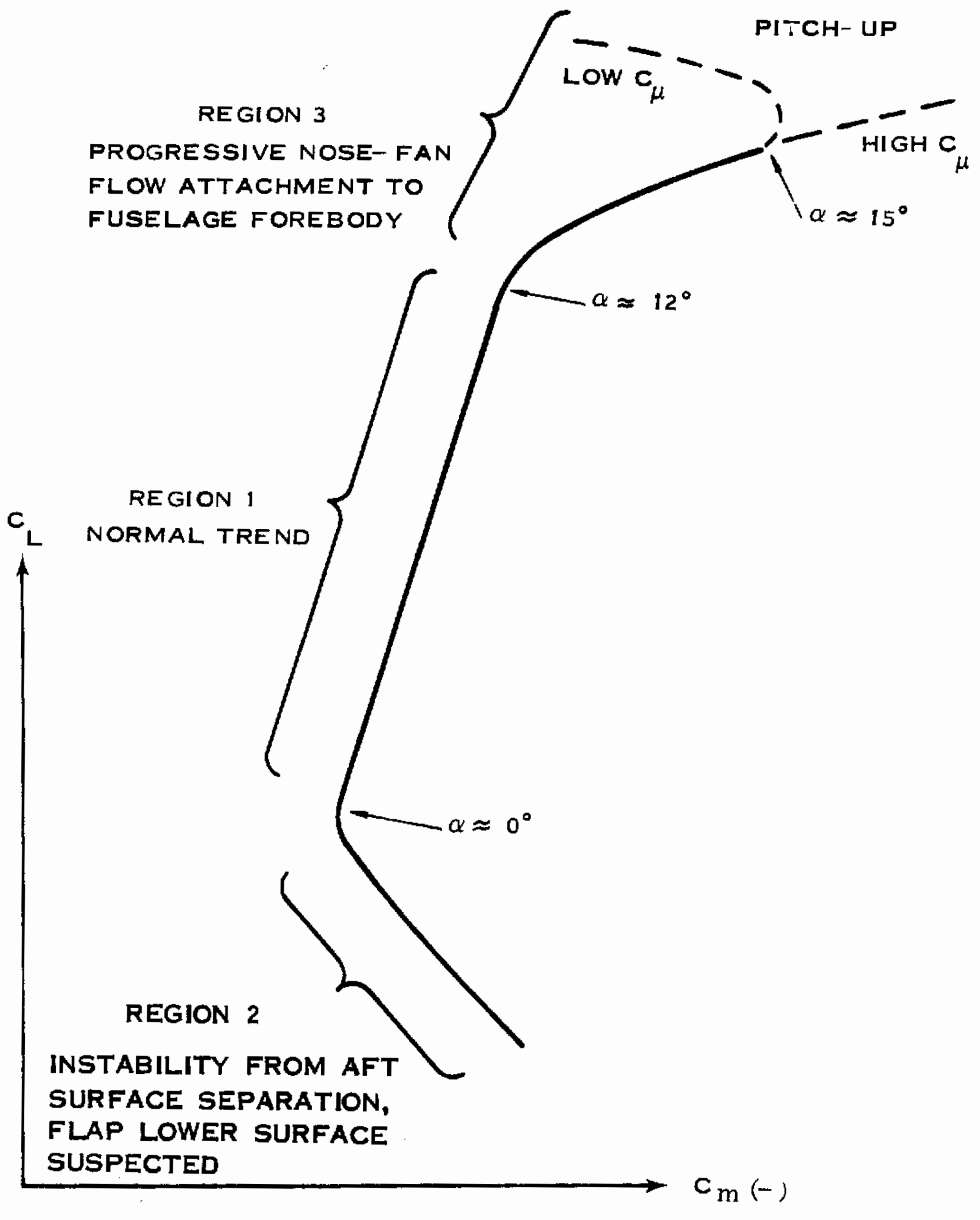

Figure 2. Sketch of Stability Regions

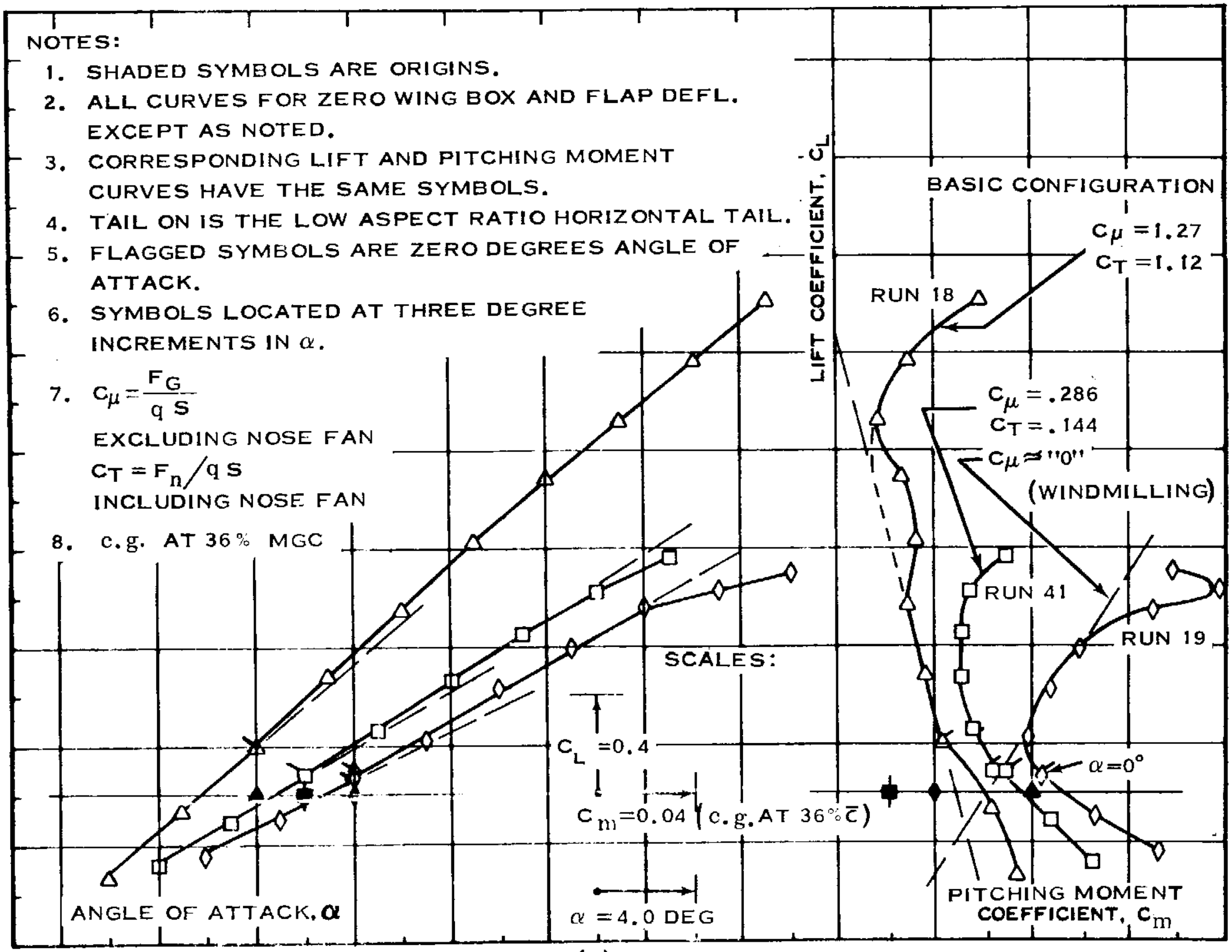

(a) TAIL ON

Figure 3. Tail On and Tail Off Stability Characteristics

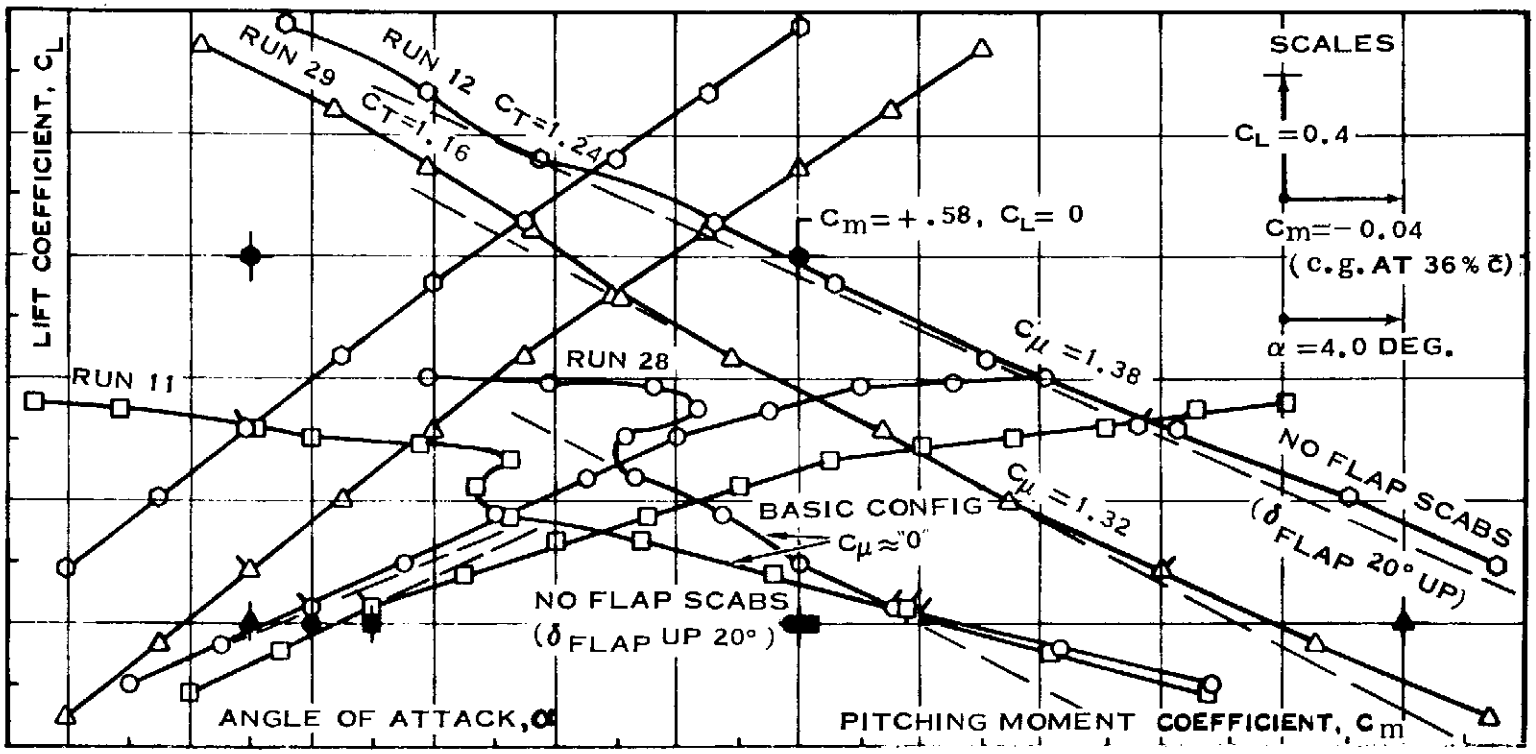

(b) TAIL OFF

Figure 3. Tail On and Tail Off Stability Characteristics (Concluded)

T.E. up), the reduced stability of region 2 applies for all angles of attack, and that in region 2, and upward deflection of the flap has no effect which is typical of separated flow. The upward deflection of the flap adds to the expansion required of the secondary fan flow. Other evidence of lower surface flap separation consists of the change in upwash at the horizontal tail below $\alpha = 0°$, for low values of C_μ, as shown in Figure 4. It was also found that the spanwise velocity distributions in the primary exits were not uniform and may have been a contributing factor. Later tests reported in Parts III and IV used screens and redesigned pipes to improve flow distribution. If lower surface flap separation proves to be the case in spite of these improvements, then a change in flap and lower surface lines can be used to avoid separation.

The stable change in pitching moment curve slope and reduced C_{L_α} of region 3 is believed to be a nose fan effect. Tuft observations indicated that, with q = 0, the nose fan exhaust appeared to be separated from the fuselage. With this in mind, tufts were put on the lower surface of the fuselage, and for run 12, tufts showed a gradual attachment of nose fan exhaust flow starting at $\alpha = 15°$ and becoming complete at $\alpha = 30°$. This gradual attachment to the lower surface with increasing angle of attack would result in increasingly negative pressure increments on the lower forward fuselage, affecting a stable change in moment curve slope. As might be expected, runs 18 and 19 of Figure 3 show that this effect is gradual for high values of C_μ and more abrupt for low values of C_μ. There was speculation that such a stable change may be due to a partial stall of the nose fan. However, RPM during the run was steady indicating no unloading of the nose fan.

The tail-on data of Figure 3 are for the low aspect ratio horizontal tails. The high aspect ratio horizontal tails were also tested. Results in pitch are shown in Figure 5 for both the low and high aspect ratio horizontal tails at two different positions provided by the boom extension. Although more stable at low angles of attack, the high aspect ratio tail exhibits indication of stalling (see Section III, Figure 6). Unless otherwise noted, tails are in the forward position without the boom extension.

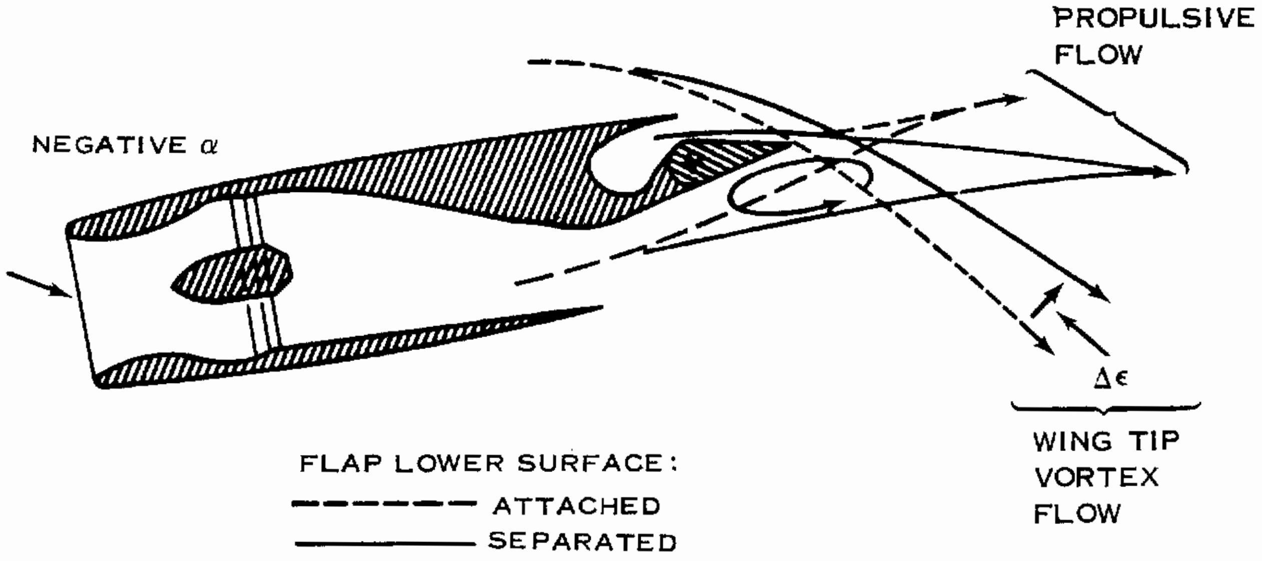

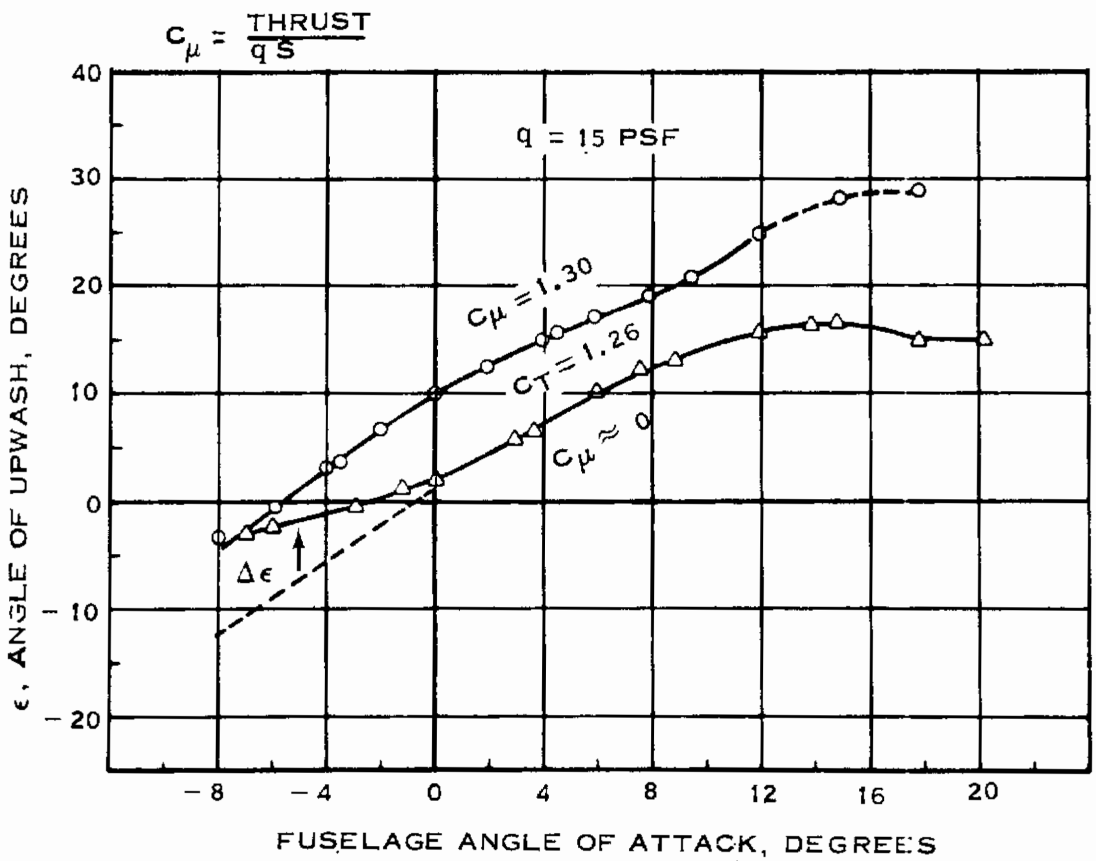

Figure 4. Effect of Thrust Level on Upwash

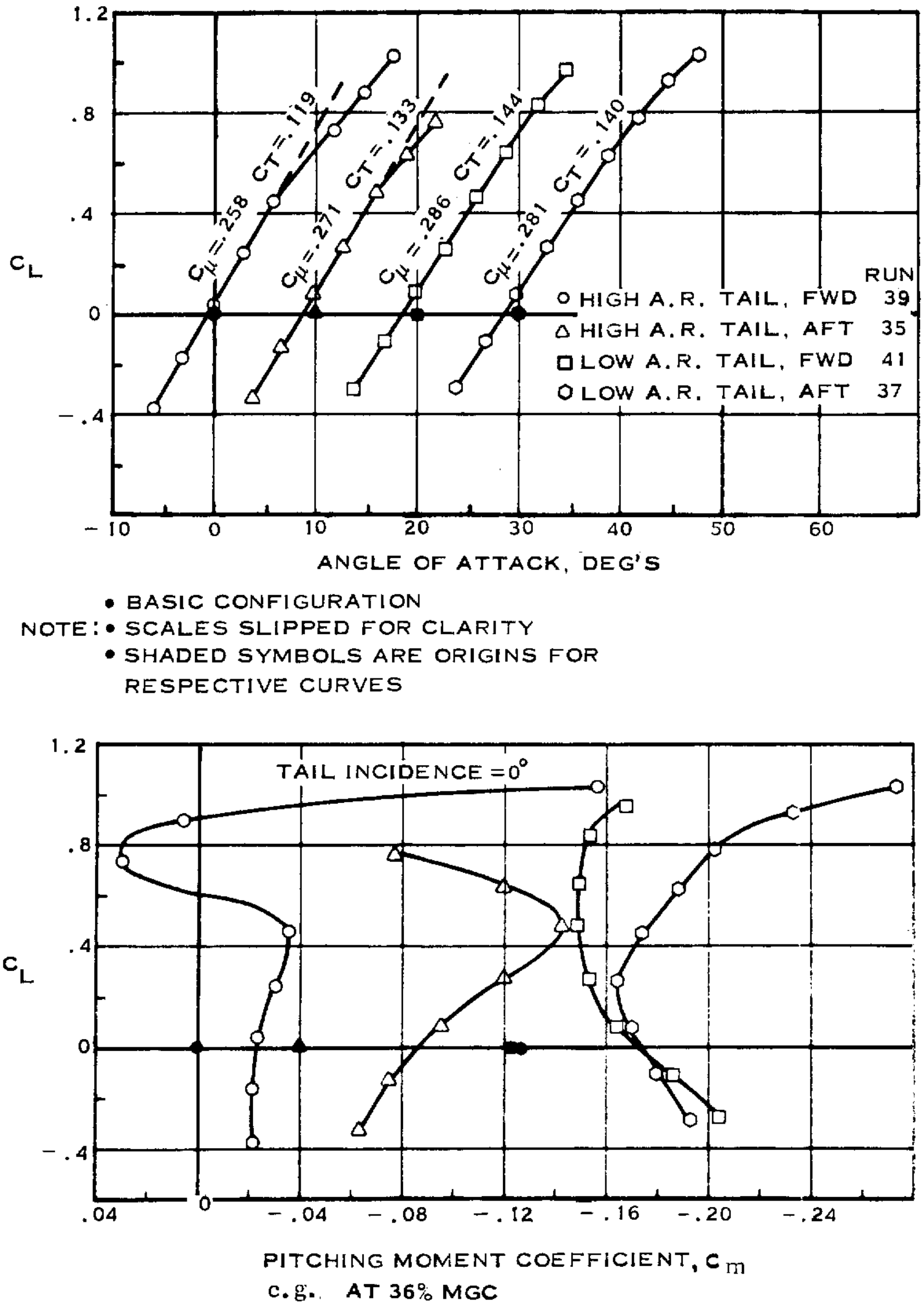

Figure 5. Effect of Horizontal Tail Planform and Location

SECTION III

LONGITUDINAL CONTROL

Longitudinal control effectiveness runs were made for the high aspect ratio tail on the semi-span model at a $C\mu$ of approximately .72 and for the low aspect ratio tail on the full-span model at $C\mu = 1.30$ and $C\mu \approx$ "0." These three sets of curves are presented Figures 6, 7, and 8. Figure 6 again shows the pitch-up due to horizontal tail stall which is indicated by the cross-over or merging of curves at both low and high angles of attack. Figure 6 also shows the unstable change in slope in region 2 associated with flap lower surface separation. It is also noted that the stable change in slope at high angles of attack that exists for the nose-fan equipped, full-span model was not present for earlier tests of the semi-span model. $C_{m_{i_t}}$ for the high aspect ratio horizontal tail is -0.0088.

Low aspect ratio horizontal tail effectiveness presented in Figures 7 and 8 shows that $C_{m_{i_t}}$ is not affected by these ranges of $C\mu$ and has a value of approximately -0.0054. There seems to be considerable inconsistency in the pitching moment data for the various tail incidences of Figures 7 and 8; therefore, a liberal amount of fairing was done in order to get a reasonable family of curves for computation of the downwash presented in Figure 4, and tail incidences required to trim which are presented in Figure 9. The fact that the tail-on curves of Figures 7 and 8 do not cross-over or merge with each other indicates that the tails are unstalled even though tufts indicate disturbed flow which may portend airframe buffet. The three stability regions discussed under Longitudinal Stability are evident in Figures 7 and 8, and, in addition, there is a reduction in stability at $C\mu = 1.30$ and high angle of attack which exists for large negative tail incidence only. This is believed to be due to unporting between the base of the horizontal tail and tail boom. The same unporting effect should exist for $C\mu \approx$ "0" in Figure 8, but the forward shift in a.c. position already existing above $\alpha = 15°$ for all incidences, and lack of some data points at high angles of attack, makes the effect difficult to see.

Trim curves for the full-span model and low aspect ratio horizontal tail are presented in Figure 9. The nonlinearities of the curves at low and high angles of attack have been attributed previously to flap lower-surface flow-separation and nose fan flow attachment. The trim change due to power ($\Delta i_t = 15°$) is a function of flap setting. A down rigging of the flaps would seem to improve the lower surface flow separation characteristics and the longitudinal trim change due to power. A nominal flap deflection of 10 degrees is recommended for use in the high speed wind tunnel program.

SEMISPAN MODEL
LTV LSWT TEST 172
ZERO WING BOX AND FLAP DEFL.
$W_a \approx 16.5$ LB/SEC ($C_\mu \approx .72$, $C_T \approx .72$)
REF. AREA FOR THIS DATA DOES NOT INCLUDE HORIZONTAL TAILS – ALL OTHER PLOTS FOR FULL-SPAN DO HAVE HORIZONTAL TAILS INCLUDED.

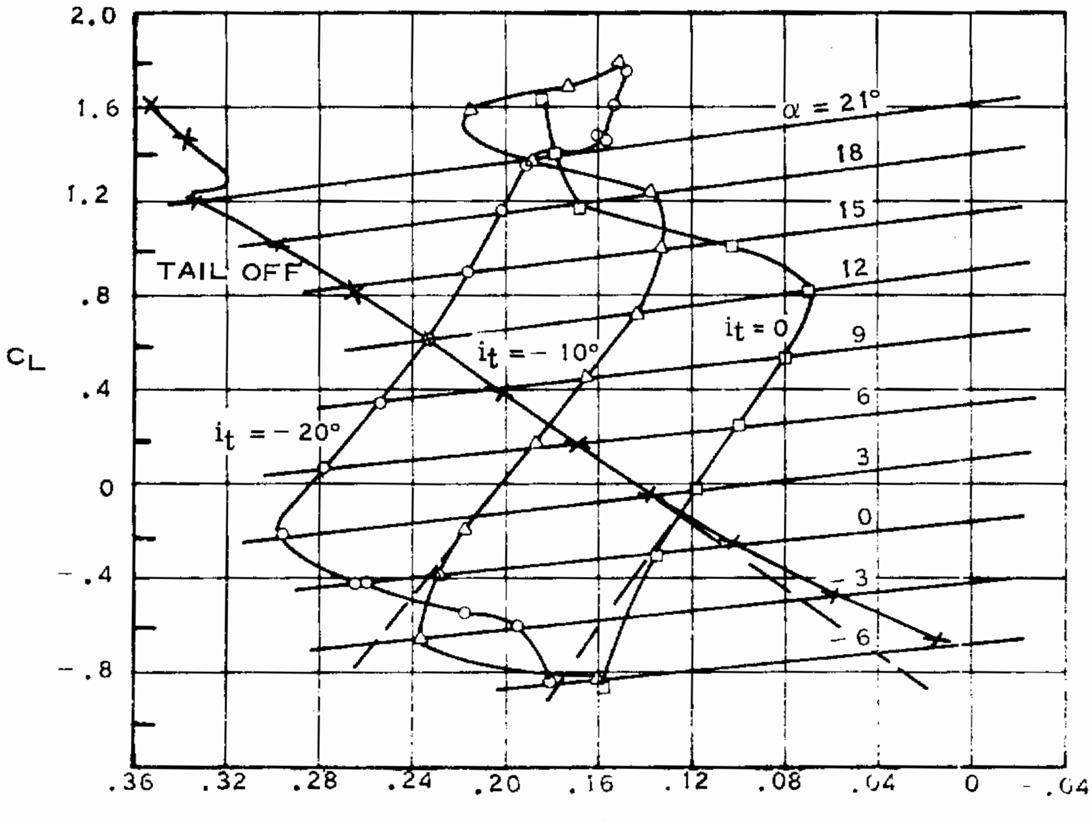

$C_{m_{i_t}} = -0.0088$

$\left(\frac{\ell_t}{\bar{c}}\right)_{AERO} = 0.94$ AVE.

SEMI-SPAN MODEL

$\frac{S_W}{S_{W+T}} = 0.95$

Figure 6. High Aspect Ratio Horizontal Tail Effectiveness

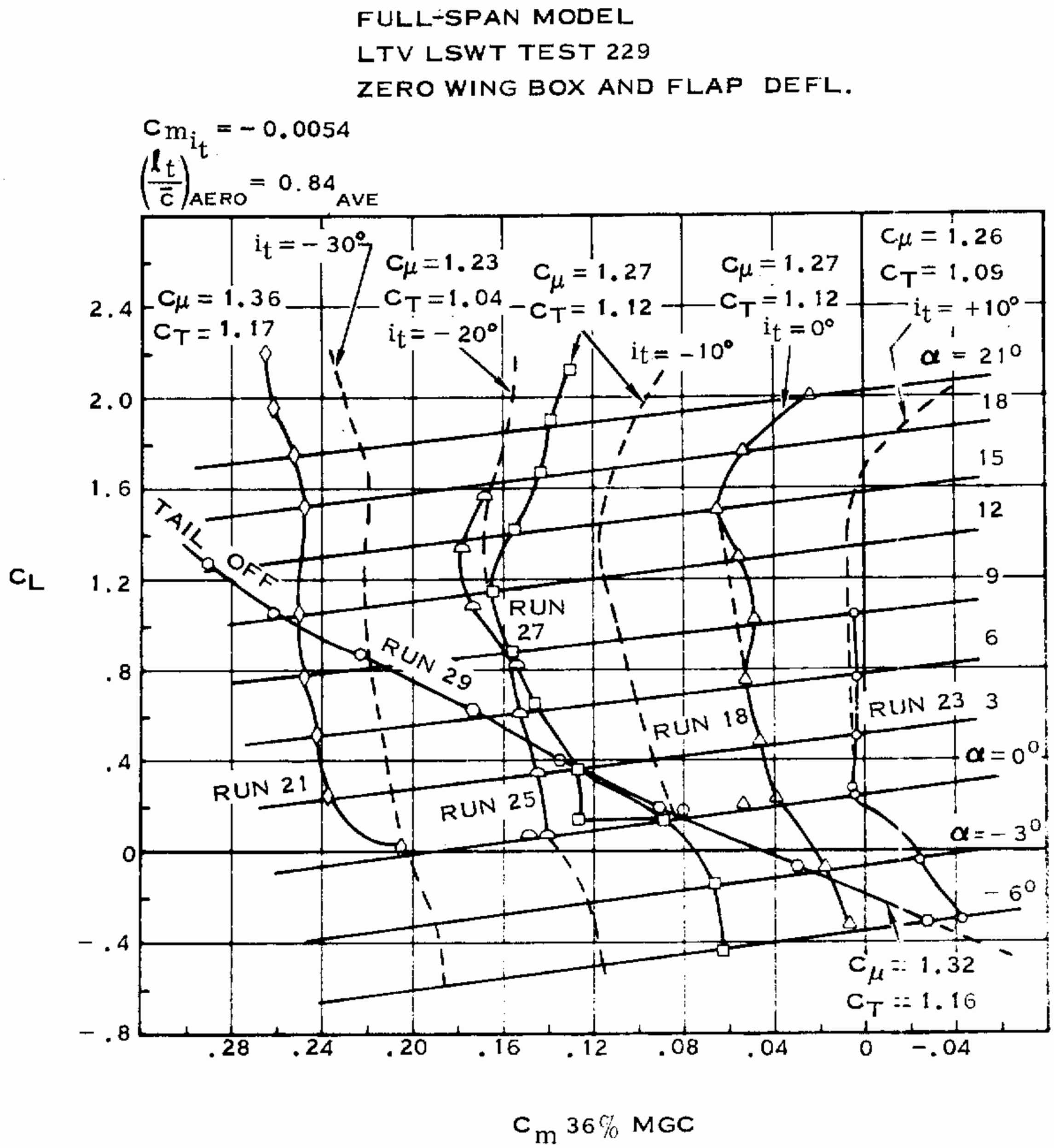

Figure 7. Low Aspect Ratio Horizontal Tail Effectiveness C_μ = 1.27

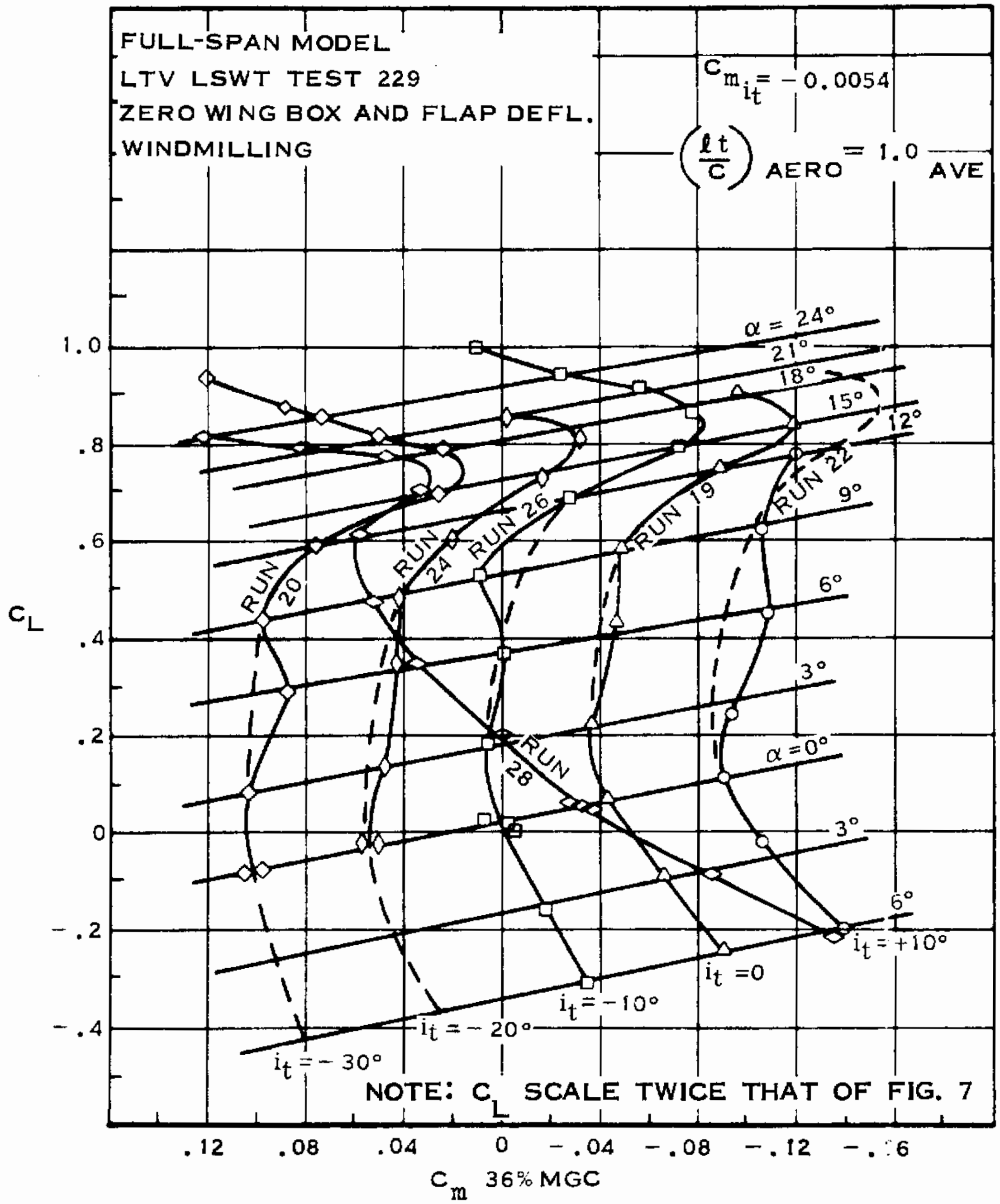

Figure 8. Low Aspect Ratio Horizontal Tail Effectiveness $C_\mu \approx$ "0"

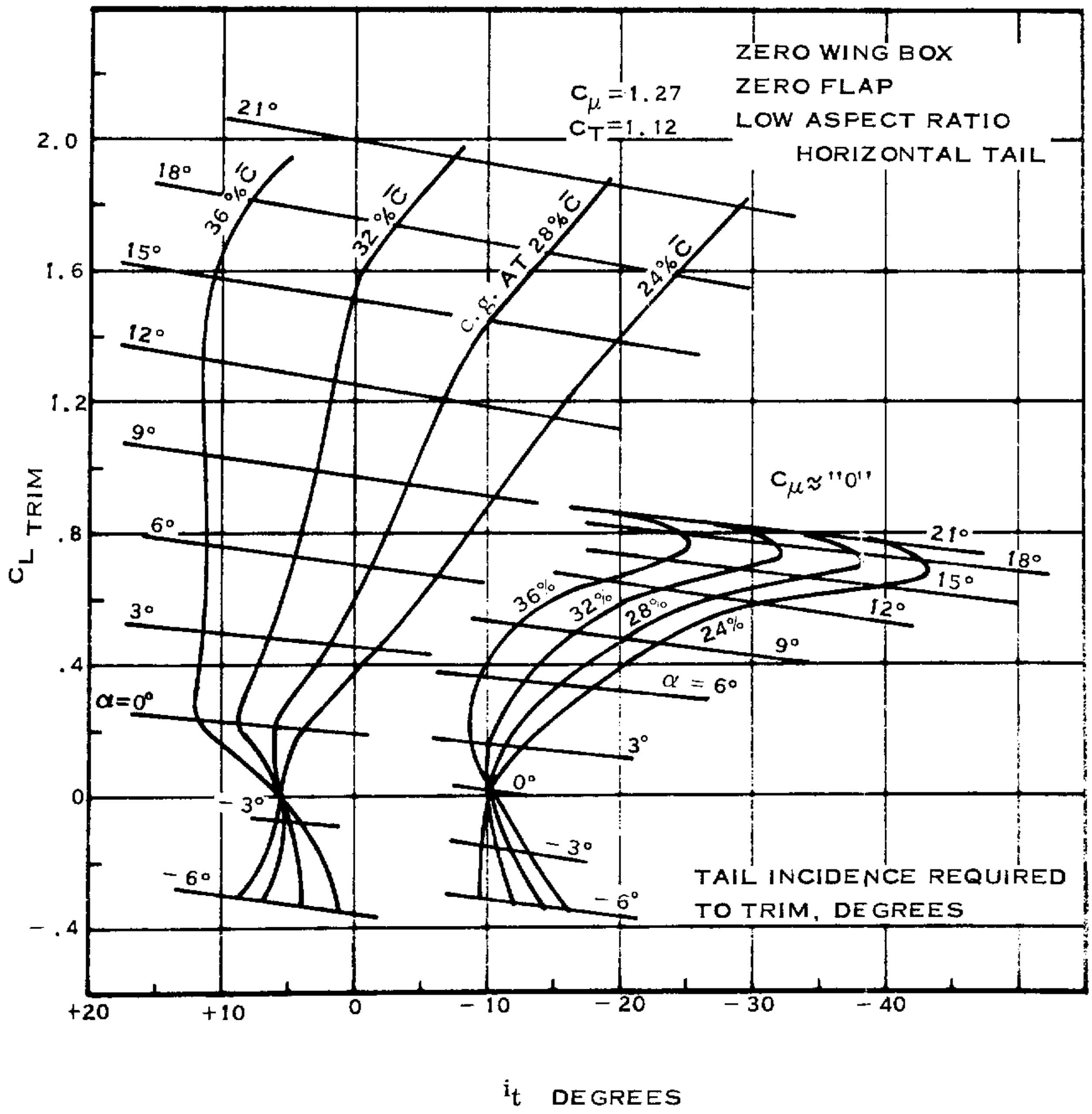

Figure 9. Tail Incidence Required to Trim vs $C_{L_{TRIM}}$

The horizontal tail contributes to the airplane span efficiency by increasing overall wing span and influencing the spanwise lift distribution to be more elliptical. Therefore, Figure 10 is included to show the increment in lift attributable to the horizontal tail. Within the ranges tested, the low aspect ratio horizontal tail shows no indication of stall.

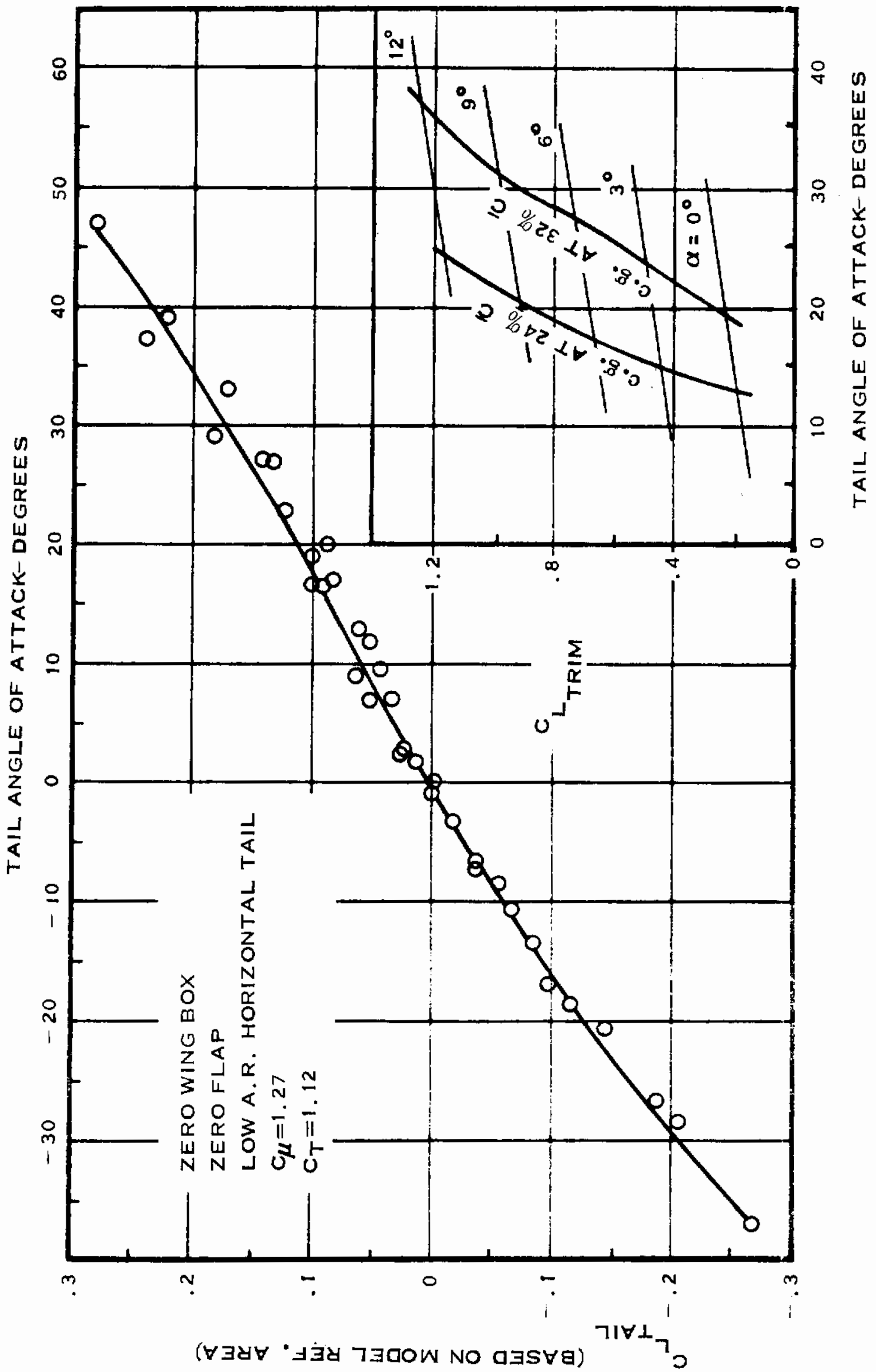

Figure 10. Low Aspect Ratio Horizontal Tail Lift and Trim Characteristics

20 is blank

SECTION IV

DIRECTIONAL STABILITY

Figure 11 presents tail-on yawing moment curves with tail location and horizontal tail planform as parameters. Tail-off yaw runs were not made during the full-span shakedown test. Tufts indicate varying degrees of disturbed flow on the vertical tails even at zero yaw due to the strong wing tip vortex and resulting high sidewash. The angle of attack is three degrees, $C_L = 0.28$, and the wing tip vortex is of moderate strength. Although the results indicate a directionally unstable configuration (with nose fan), the effects of tail location and horizontal tail aspect ratio are normal: a longer tail arm provides more tail contribution to stability and the higher aspect ratio horizontal tail provides more tail contribution by additional end plating of the vertical tail and by moving the sidewash from the wing tip vortices further outboard. Without benefit of tail-off data, the nonlinearities in the C_η curves at $\psi = +5$ and $-10°$ cannot be explained.

Figure 12 shows that the effect of power on directional stability at low angles of attack is slight for the range of powers tested. The effect of the nose fan is significant, however, as shown in Figure 13(a), which compares the nose fan at two RPM's with the plugged nose. The computed stability decrement due to mass flow through the inlet is $\Delta C_{n\psi} = +0.0036$ which is close to that observed between runs 4 and 30. The fact that the plugged nose configuration had an asymmetric tail arrangement makes the comparison approximate. The differences between the curves for $C\mu \approx$ "0" and $C\mu = 1.30$ at this angle of attack is not explained. Contrary to what is shown, a reduction in stability at high $C\mu$ would be expected. This, and the unusual shape of run 31 compared to run 30 and those of Figure 12, makes run 31 appear to be of doubtful validity. Therefore, it is believed that power effects on directional stability are small at high angles of attack also. Figure 13(b) presents the side force variations for the same runs, and shows that $C_{Y\psi}$ is about the same for the nose fan and the plugged nose. Therefore, the increase in directional stability due to plugging the nose represents a rearward shift in center of pressure. Refer to Figure 1(b) for a description of the plugged nose configuration. Figure 14 presents a comparison of two yawing moment curves at different angles of attack and values of $C\mu$. If the effects of power can be assumed to be small (as indicated by Figure 12), then directional stability is independent of angle of attack, in spite of the increasing wing tip vortex strength. There were no data available for direct comparison of angle of attack effects at constant power.

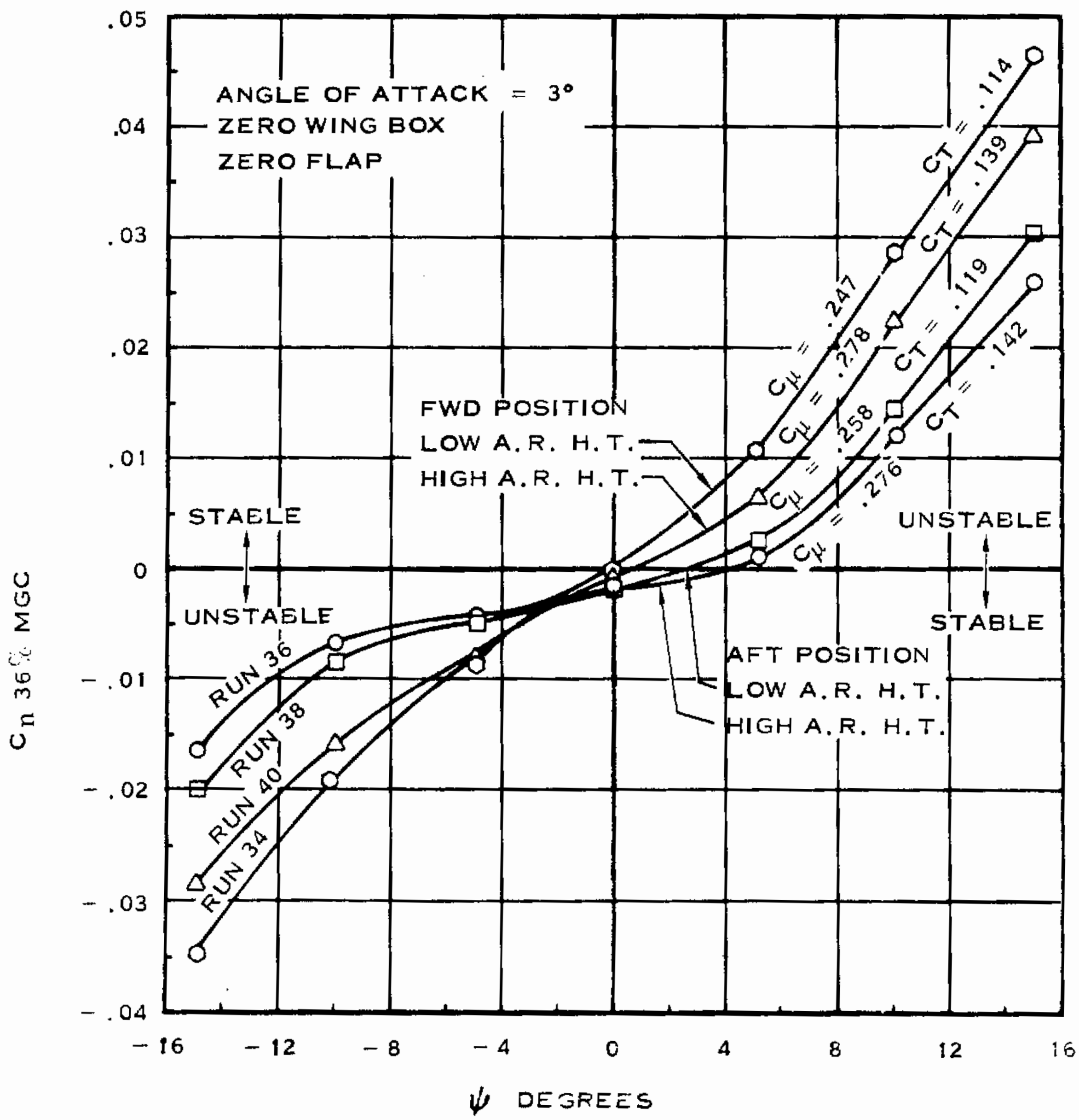

Figure 11. Effect of Tail Location and Horizontal Tail Planform on Directional Stability

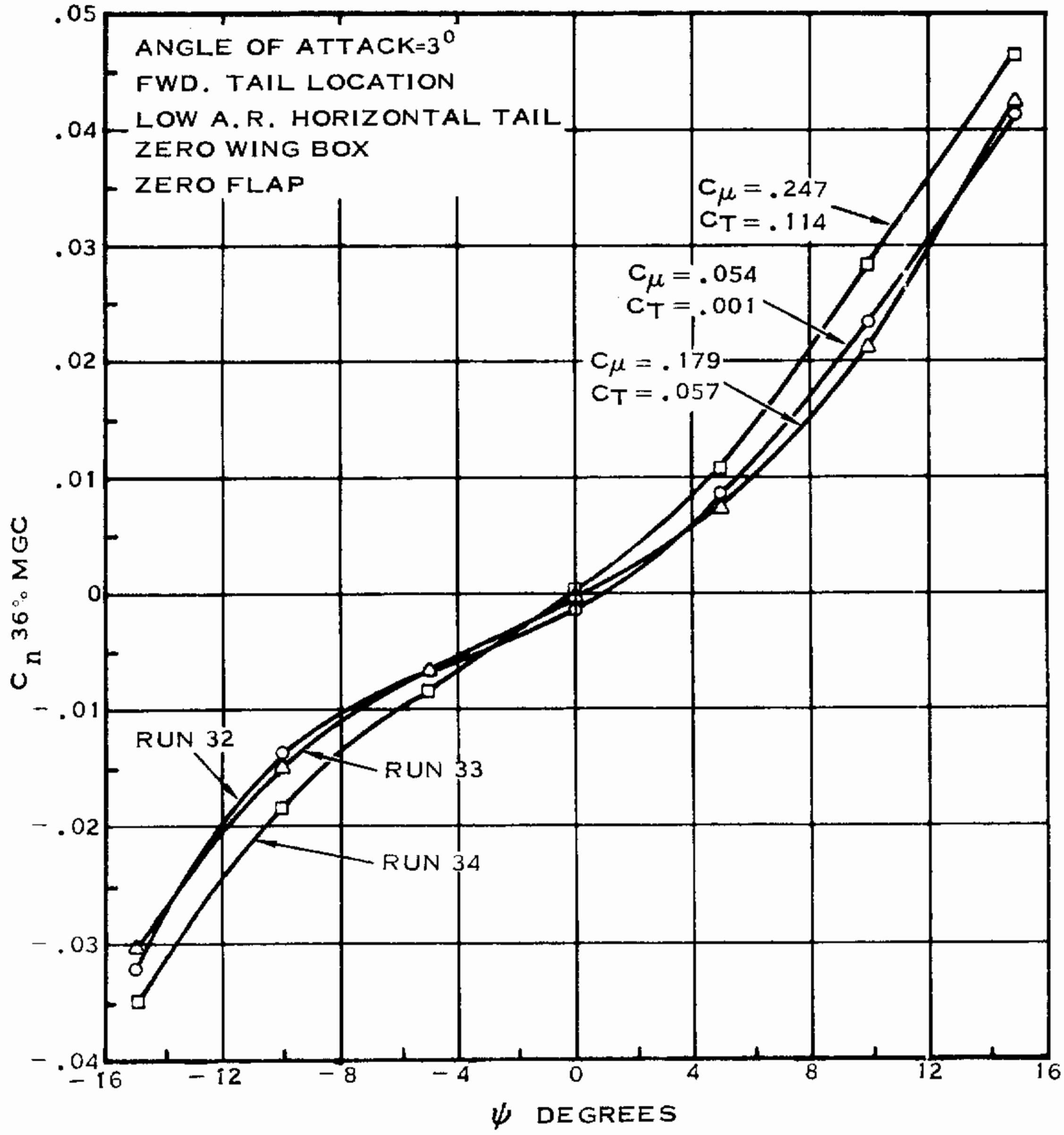

Figure 12. Effect of Thrust Level on Directional Stability

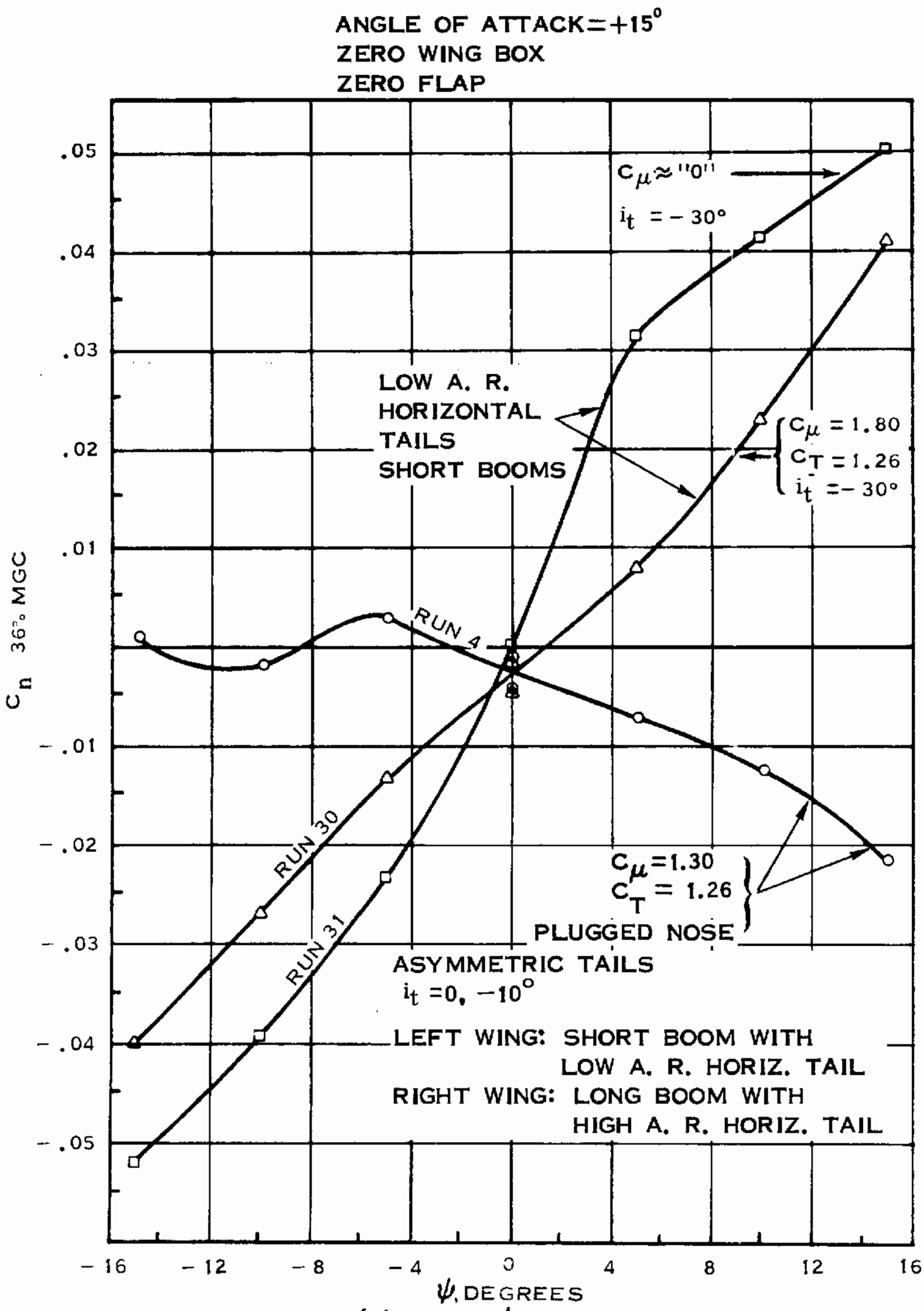

(a) C_n VS ψ

Figure 13. Effect of Plugged Nose on Directional Stability

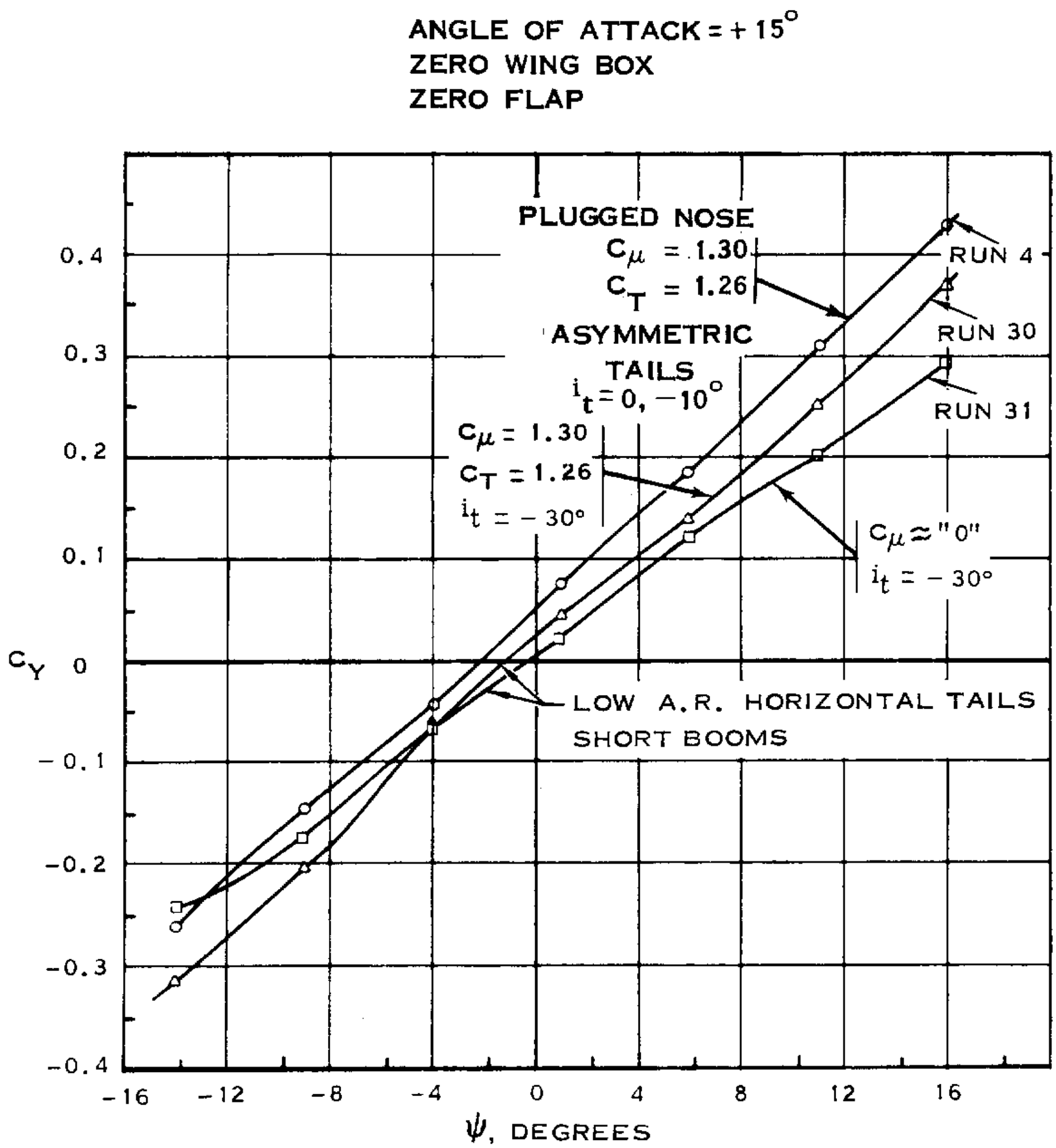

(b) C_Y VS ψ

Figure 13. Effect of Plugged Nose on Directional Stability (Concluded)

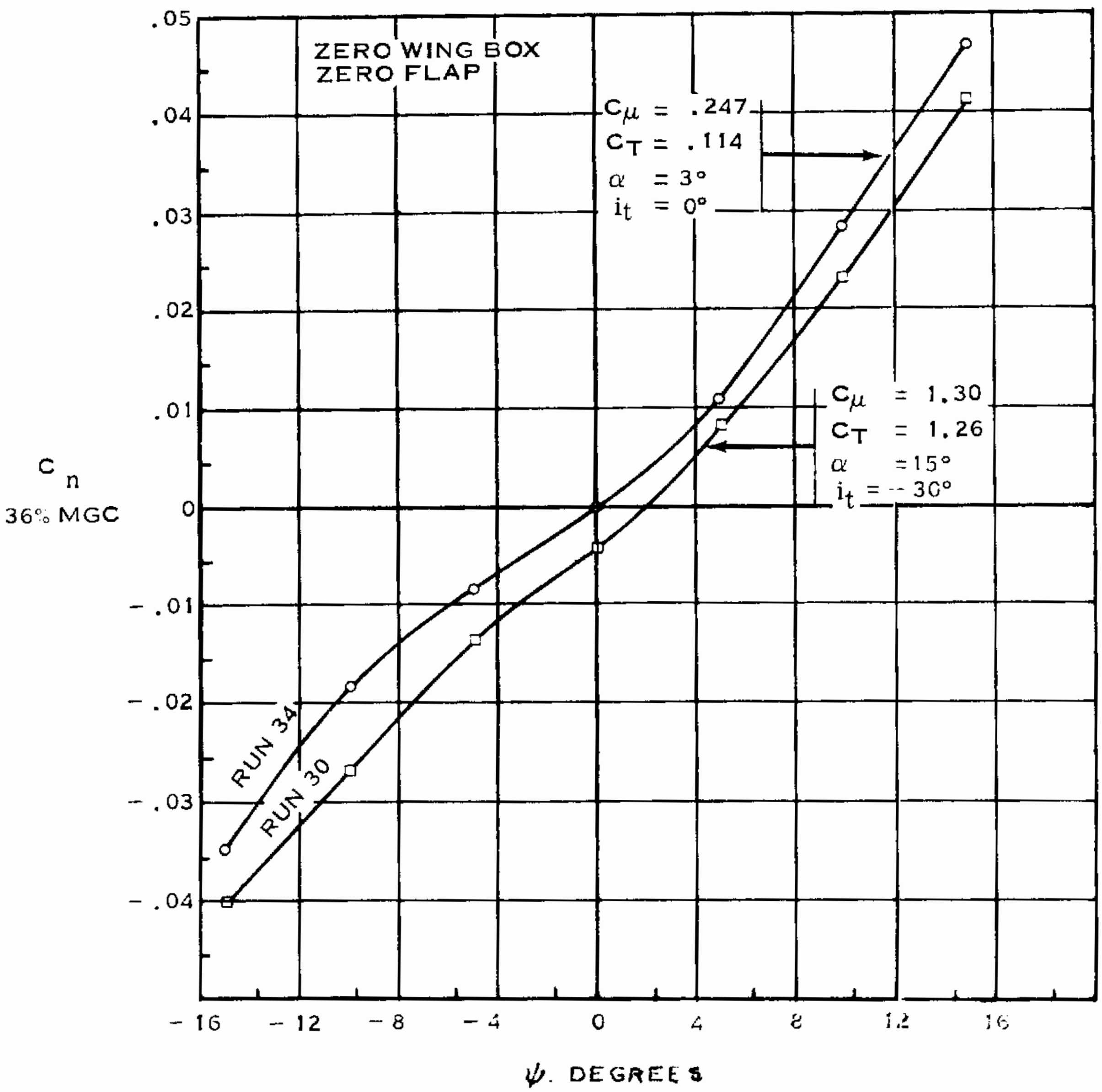

Figure 14. Effect of Angle of Attack on Directional Stability

To provide an indication of the degree of directional instability, Figure 15 is included that shows the forward c.g. shift required to produce adequate stability, based upon the stability levels presented in Figure 11. For neutral directional stability, a forward c.g. shift to 27% MGC is required for the tails in the forward position (with low A.R. horizontal tail), which compares with a 36% MGC longitudinal neutral point from Figure 9, indicating that the configuration is considerably less stable directionally than longitudinally in the cruise mode. Recent results from the Langley 17-foot low speed tunnel indicate that a centerline vertical tail should be incorporated, perhaps in addition to outboard tails.

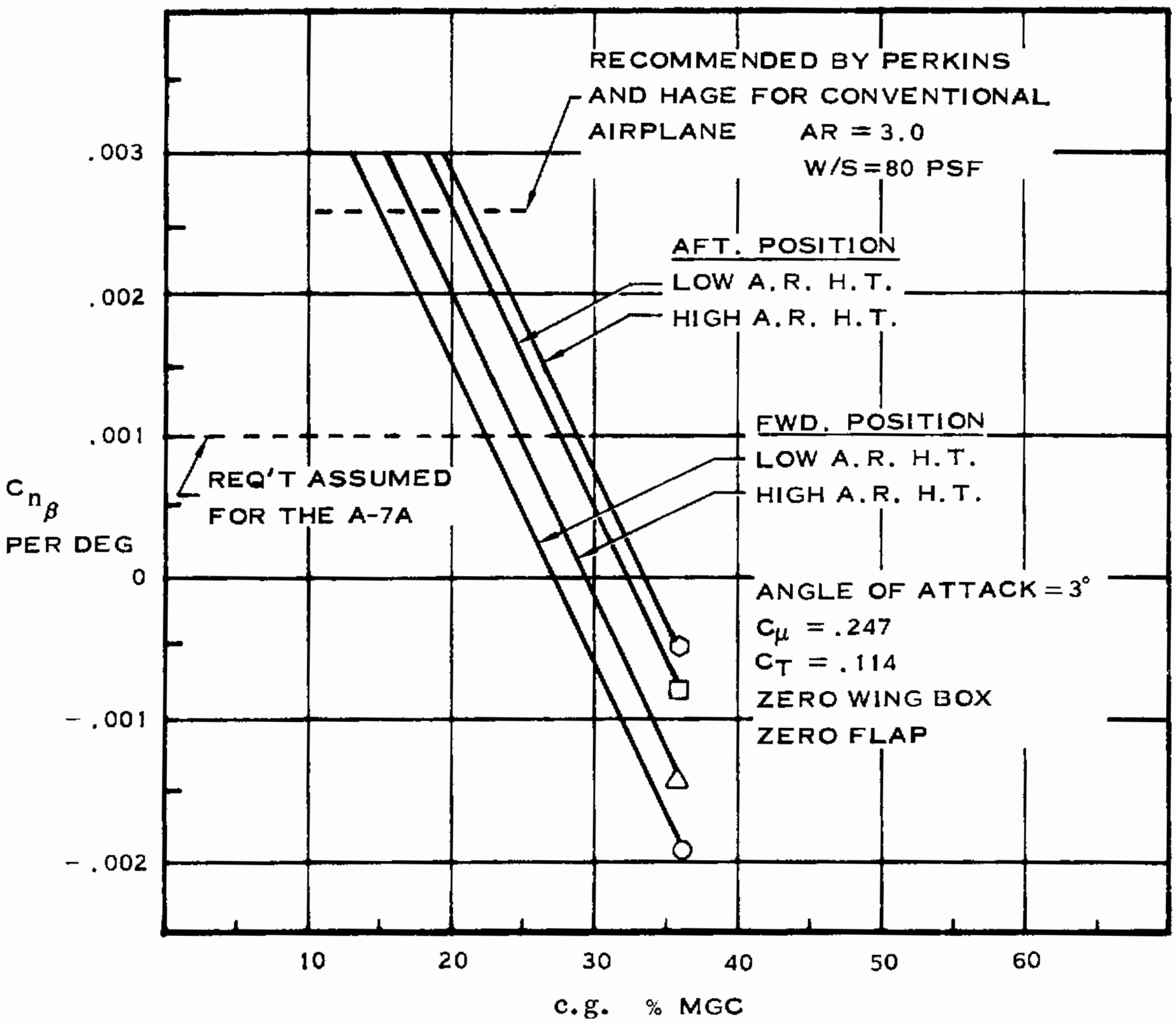

Figure 15. Directional Stability Change with c.g. Location

SECTION V

LATERAL STABILITY

For all the configurations and runs tested, the model exhibited a positive dihedral effect. Figure 16 shows that lateral stability is independent of moderate C_μ changes at low angles of attack. At high angles of attack a comparison of runs 30 and 31 of Figure 17 shows a change in C_{ℓ_ψ} with C_μ; however, in this case the C_μ change is much greater and contains the special case of windmilling fans. Figure 17 also shows that the effect of the plugged nose on C_{ℓ_ψ} is minor. Run 31 with windmilling fans ($C_\mu \approx 0$) has a much reduced value of C_{ℓ_ψ} at low values of yaw, indicating that the windmilling fan produces a poor flow condition, such as duct spillage, which affects C_{ℓ_ψ} within sideslip angle of ±4°. It is not known whether this effect is due to forces on the nose itself or an interference on downstream surfaces. Figure 18 presents a remaining comparison of runs 30 and 34, which are different in both angle of attack and C_μ. If C_{ℓ_ψ} is independent of C_μ, then Figure 18 shows the effect of angle of attack, which is believed to be the case.

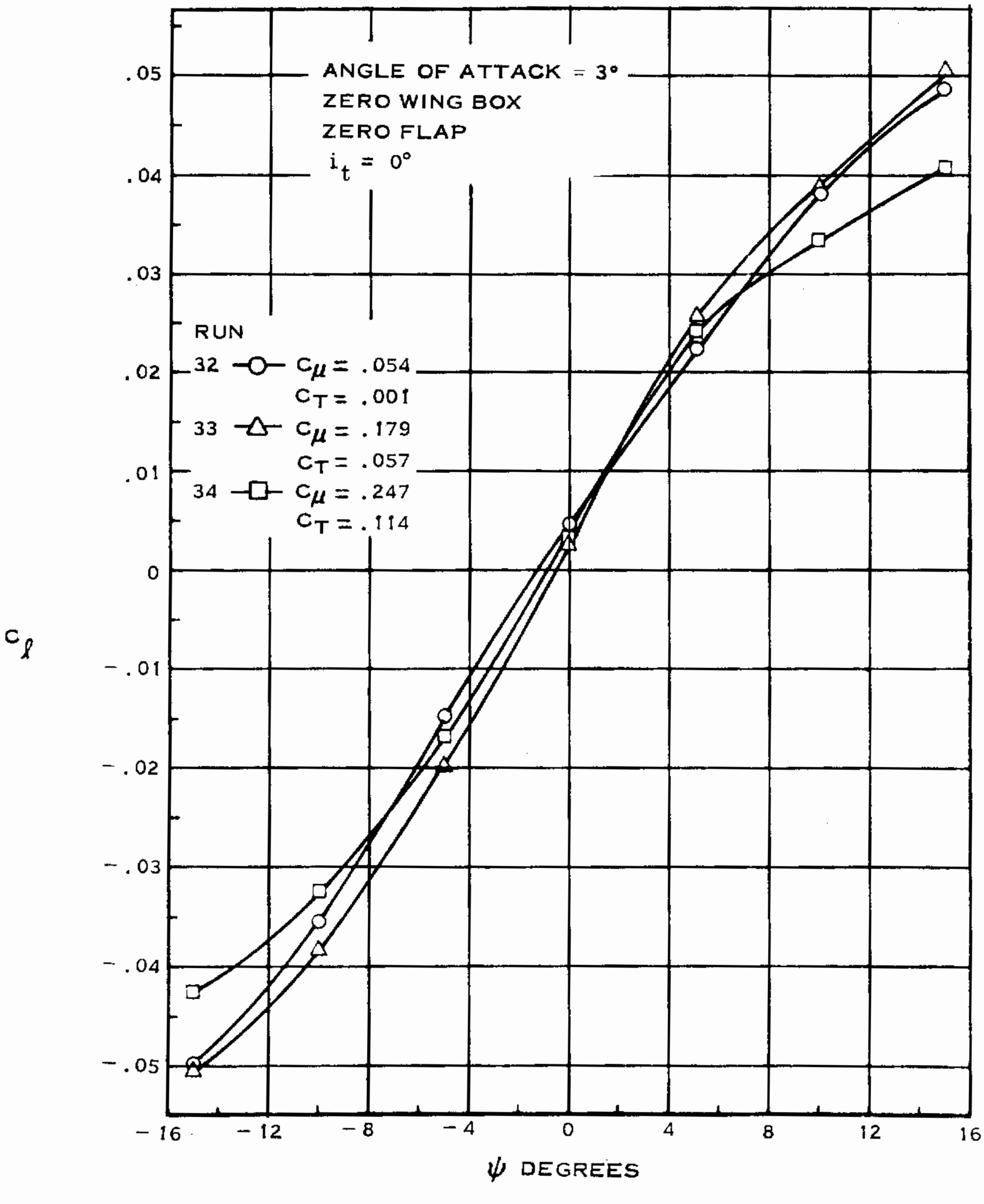

Figure 16. Effect of Thrust Level on Lateral Stability

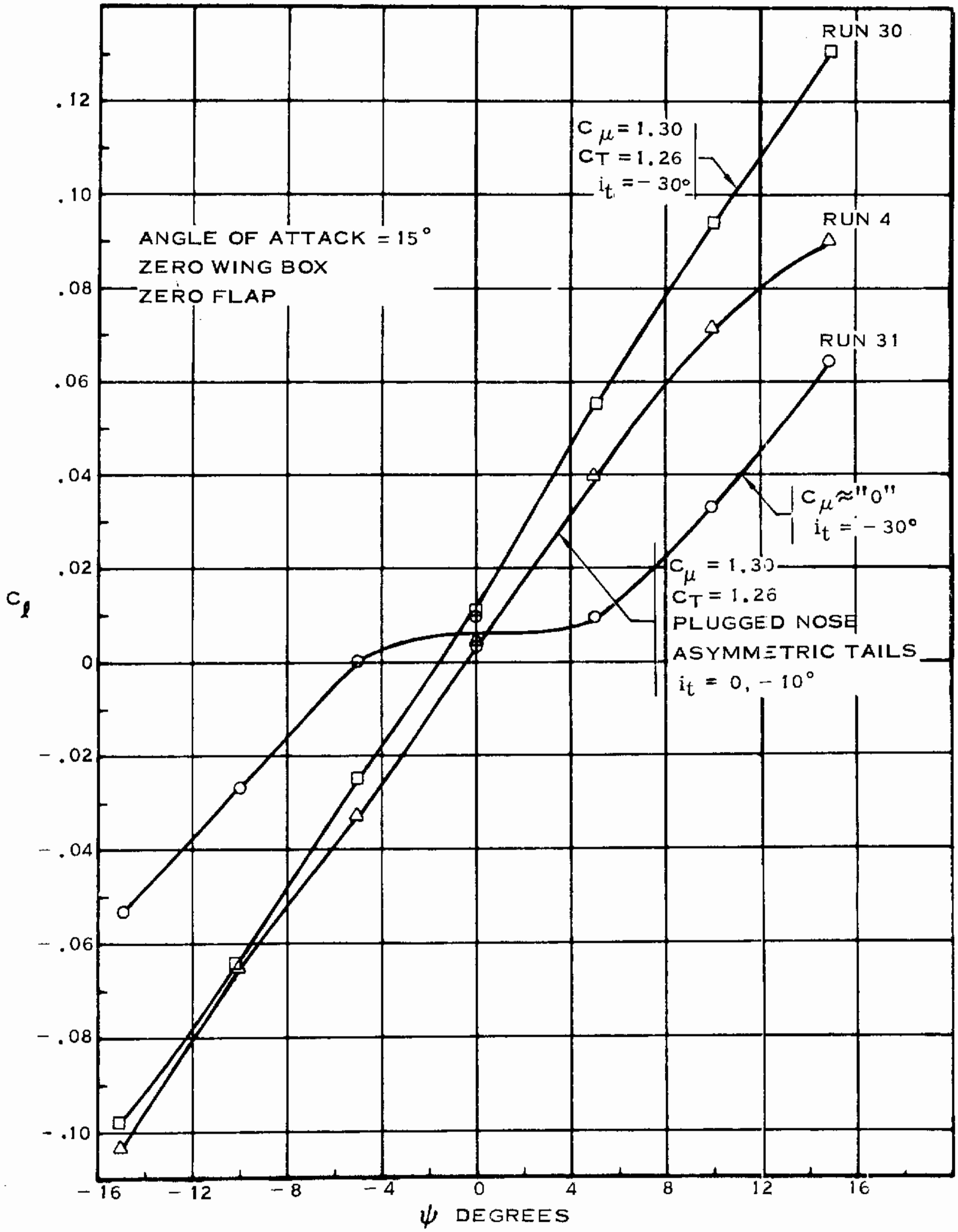

Figure 17. Effect of Plugged Nose and Thrust Level on Lateral Stability

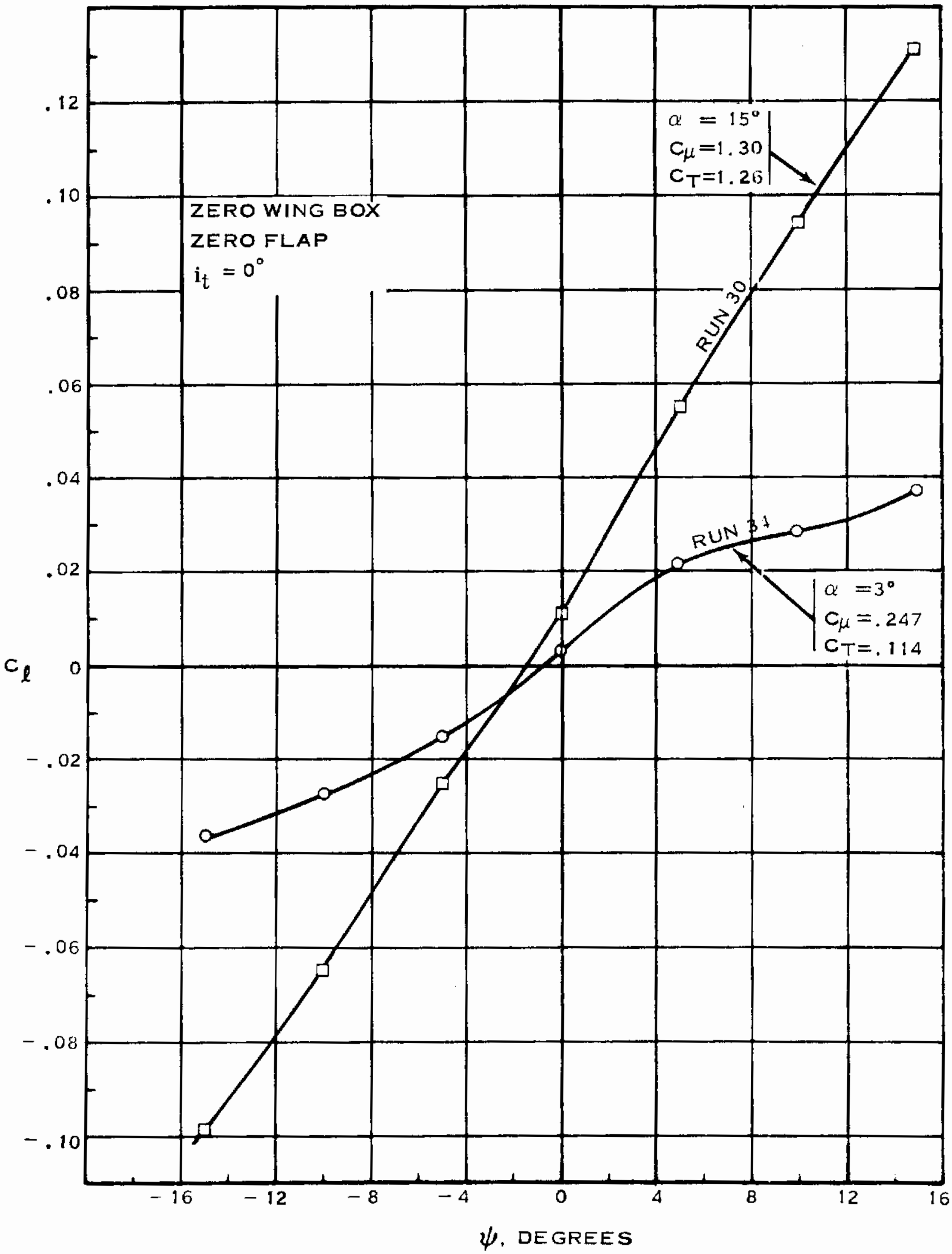

Figure 18. Effect of Thrust Level and Angle of Attack on Lateral Stability

SECTION VI

CONCLUSIONS AND RECOMMENDATIONS

The conclusions developed in the preceding paragraphs are as follows:

1. The nonlinearity of the pitching moment curves may be improved by improving the primary flow distribution and the flap contour, deflecting the flap T.E. down, and developing the nose-fan exit geometry.

2. Low aspect ratio horizontal tails are preferred over the high aspect ratio horizontal tails because tail lift is maintained avoiding pitch-up due to tail stall.

3. The control effectiveness of both low and high aspect ratio horizontal tails is adequate at the present stability levels. Longitudinal stability with low aspect ratio horizontal tails in the forward location is satisfactory for c.g.'s forward of 36% MGC.

4. Disturbed flow on the tails due to the wing tip vortex may result in buffet.

5. Directional stability is independent of angle of attack.

6. Lateral stability is affected by angle of attack.

7. Lateral stability is independent of $C\mu$ at low angles of attack, and varies with $C\mu$ at high angles of attack.

These tests provide some stability and performance characteristics of the present ADAM II configuration. In order to define configuration changes to improve the stability and performance, it is recommended that additional tests be conducted designed to investigate the flow conditions on and around the wing.

APPENDIX
RUN SCHEDULE FOR TEST NO. 229
IN LTV LOW SPEED WIND TUNNEL

RUN NO.	CONFIGURATION	q PSF	q_{SET} (IN. H_2O)	α (DEG)	ψ (DEG)	BARO PRESS (IN. Hg)	TEMP (°F)	TUFTS	δT	δF F_1/F_3	δN	NORM RPM	i_V V_1	i_V V_2	i_H H_1	i_H H_2	STATIC TARE	TRAP PRESS PSI	REMARKS	DATE 1966	ENG.
1-1	$N_2WF_1F_3T_1I_1V_1V_2H_1H_3$	0	0	0	0	29.89	49	On	0	0	0	30,000	2.5	0	-10	0	-	445	RUNS 1 THRU 10 ARE	12/2	CRP
1-2							50					21,700						460	CALIBRATION RUNS		
1-3												20,000						448			
1-4												15,000									
1-5						29.90						10,000						440			
1-6												25,000						415			
2-1		15	2.32			29.92	43					30,000						445			RHO
2-3							42					25,000						450			
2-4												20,000						442			
2-5												15,000						435			
3-1	N_3			-6/+30		29.94	41				Tare	10,000					3	430			
3-2						29.96	45					22,000					3	425		12/3	HAH
3-4				+15	-15/+15	29.98	45					20,000					4				
105		0	0	0	0	29.92	58			✓		20,000					--	380	No Data Taken		RHO
205-1		15	2.32			29.89	50			0/0		--					--	365			
-2										30/30		--									
-3										60/60		--									
-4										0/0		--									
-5										30/30		--									
-6						29.90	52			45/0		--									
5-1										0/0		20,000					--	385			CRP
-2												20,000									
6-1	N_1					29.89	51				90	30,000						390			
-2												10,000						350			
-3												25,000									
-4												15,000									
-5												20,000									

36 is blank

APPENDIX
RUN SCHEDULE FOR TEST NO. 229 IN LTV LOW SPEED WIND TUNNEL

RUN NO.	CONFIGURATION	q PSF	q_{SET} (IN. H_2O)	α (DEG)	ψ (DEG)	BARO PRESS (IN. Hg)	TEMP. (°F)	TUFTS	δT	δF F1/F3	δN	NORM RPM	i_V V_1	i_V V_2	i_H H_1	i_H H_2	STATIC TARE	TRAP PRESS PSI	REMARKS	DATE 1966	ENG.
7-1	$W^{90}_{90} N_1 F_1 T_1 I_1 V_1 V_2 H_1 H_3$	0	0	0	0	29.35	68	ON	0	60	0	30,000	2.5	0	-10	0	-	400		12/6	CRP
-2							67					25,000						395			
-3												20,000						392			
-4										90		15,000						388			
-5												20,000									
-6						39.34				60		15,000						378			
-7												10,000						368			
-8										90											
8-1	H_3	15	2.32			29.32	79			60		30,000						397			
-2						29.27						25,000						386			
-3												20,000						392			
-4												15,000						397			
-5												10,000						400			
9-1	W^{60}_{60}					29.25	80			30		15,000						300			JWH
-2												12,500									
-3												10,000									
10-1	W^{30}_{30}					29.28	75	TAIL				30,000						400			RHO
-2												10,000									
-3												25,000									
-4												15,000									
-5												20,000									
*11	$W\ N_2 F_1 T_1 I_1 V_1$			-6/+30		29.87	47	NOSE		-0		WM	2.5		OFF		11	0		12/3	
12						29.86	45					20,000						427			
*13	H_1					29.83		OFF				WM			+10		13	0			
14							42					20,000			+10			400			
15								VHT				WM			-30			0			
16												20,000			-30			375			
17						29.81						WM			0			0			
18				-6/+21		29.41	72					20,000						400	Flap Scabs On		CRP

38 is blank

APPENDIX
RUN SCHEDULE FOR TEST NO. 229
IN LTV LOW SPEED WIND TUNNEL

RUN NO.	CONFIGURATION	q PSF	q_{SET} (IN. H_2O)	α (DEG)	ψ (DEG)	BARO PRESS (IN. Hg)	TEMP. (°F)	TUFTS	δT	δF F_1/F_3	δN	NORM RPM	i_V (V_1 V_2)	i_H (H_1 H_2)	STATIC TARE	TRAP PRESS PSI	REMARKS	DATE 1966	ENG.
19	$WN_2F_1T_1I_1V_1H_1$	15	2.32	-6/+18	0	29.41	72	UHT	0	0	0	WM	2.5	0	13	0	Flap Scabs on From Here On	12/5	CRP
20				0/+30		29.40	71							-30					
21				0/+27			72					20,000				400			
22				-6/+12			71					WM		+10		0			HAH
23				-6/+9								20,000				400			
24				0/+21								WM		-20		0			
124				0/+21													Repeat of Run No. 24 with Press. Data		
25				0/+18								20,000				400			
26				-6/+27				OFF								0			
27				-6/+24										-10		400			
28						29.38						0		OFF:	11	0			
29												20,000				400			
30	H_1			+15	-15/+15		69						5.0	-30	30				
31												0				0			
*32		100	15.73	+3		29.36	78					10,000		0	32	400			
33							85					15,000							
34							84					20,000			32				
*35	$WN_1F_1T_1I_1V_2H_3$			-6/+15	0	29.25	86	TAIL		CRUISE		20,000			35	375		12/6	
*36				+3	-15/+15	29.27	87								36				
*37	H_4			-6/+18	0		86								37				
*38				+3	+15/+15		82								38		No Pressure Data Pt No. 8 No Final Zero		
39	V_1H_2			-6/+18	0	29.26	80								13	370		12/7	CRP
40				+3	+15/+15	29.28	84								32				
41	H_1			-6/+15	0	29.29	86								13	348			

40 is blank

APPENDIX

RUN SCHEDULE FOR TEST NO. 229
IN LTV LOW SPEED WIND TUNNEL

RUN NO.	CONFIGURATION	q PSF	q_{SET} (IN. H_2O)	α (DEG)	ψ (DEG)	BARO PRESS (IN. Hg)	TEMP. (°F)	TUFTS	δT	δF F_1/F_3	δN	NORM RPM	i_V (V_1 V_2)	i_H (H_1 H_2)	STATIC TARE	TRAP PRESS PSI	REMARKS	DATE 1966	ENG.
42	$WF_2T_1I_1V_1H_1$	15	2.32	0	0	29.29	80	Tail Flap	0	~	0	20000	5	0	-	400	Vary Primary Press; Data Taken at 0° Flap & 50% Stall at Each Primary Setting	12/7	CRP
43						29.27	78					15000							
44		↓	↓			↓						10000							
45		0	0	↓		29.21	↓			↓		0			↓	↓	↓		
46	↓	100	15.73	-6/+15		29.17	86			Cruise		20000	↓		13	395			
47	$WF_2T_1I_1$ H_1	15	2.32	0	↓	29.15	84	↓	↓	↓	↓	↓	Off	↓	-	400	Flaps Set at 0° & at 50% Stall	↓	↓

DISTRIBUTION LIST

Addressee	No. of Copies
Air Force Systems Command Wright-Patterson Air Force Base, Ohio 45433	
ATTN: FDP (STINFO)	1
ATTN: FDE (Library)	1
ATTN: FDMM	10
ATTN: ASNPD-30	1
ATTN: SEPDE	1
ATTN: ASB	1
ATTN: APT	1
ATTN: ARD-1	1
ATTN: AFIT (Library)	1
DDC-TIASS Cameron Station Alexandria, Virginia 22314	20
Secretary of the Air Force (SAFRD) Washington, D.C. 20330	1
Headquarters U. S. Air Force (AFRSTF) Washington, D.C. 20330	1
AFCSAI Study Information Group Assistant Chief of Staff Studies and Analysis Headquarters U. S. Air Force Washington, D.C. 20330	1
AEDC ATTN: Technical Library Arnold Air Force Station, Tennessee 37389	2
Air Force Missile Development Center Holloman Air Force Base, New Mexico 88330	1
Air University Library Maxwell Air Force Base, Alabama 36112	1
DFSLB U. S. Air Force Academy, Colorado 80840	1

DISTRIBUTION LIST (continued)

Addressee	No. of Copies
Air Force Office of Scientific Research Washington, D.C. 20325	1
Air Force Systems Command Reference 1366 CA ATTN: SCS-41 Andrews Air Force Base Washington, D.C. 20331	3
AFSC ATTN: SCTSM Andrews Air Force Base Washington, D.C. 20331	1
Office of Aerospace Research ATTN: Technical Library United States Air Force Washington, D.C. 20333	1
DOL ATTN: Technical Library Bolling Air Force Base Washington, D.C. 20332	1
AFSC STLO Langley Research Center (NASA) Langley Air Force Base, Virginia 23365	6
AFSC STLO Ames Research Center (NASA) Moffett Field, California 94035	3
Headquarters U. S. Army Material Command ATTN: AMCRD-RP-A AMCRD-DF Washington, D.C. 20315	 1 1
Chief of Research and Development Department of the Army ATTN: Physical Science Division 3045 Columbia Pike Arlington, Virginia 22204	1
Chief of Research and Development Department of the Army ATTN: Air Mobility Division Mr. John Beebe Washington, D.C. 20310	1

DISTRIBUTION LIST (continued)

Addressee	No. of Copies
Commanding Officer U. S. Army Aviation Material Laboratories ATTN: SAVFE-PP Fort Eustis, Virginia 23604	6
Headquarters U. S. Army Research Office—Durham ATTN: Technical Library Box CM Duke Station Durham, North Carolina 27706	1
Commanding General U. S. Army Aviation Material Command Administration Services Office ATTN: AMSAV-ADR P. O. Box 209, Main Office St. Louis, Missouri 63166	3
U. S. Army Aeronautical Research Laboratory ATTN: P. F. Yaggy Moffett Field, California 94035	2
Chief of Naval Material (0314) Navy Department Washington, D.C. 20360	1
Chief of Naval Material (0331) Navy Department ATTN: Mr. H. P. Santiago Washington, D.C. 20360	1
Commander Naval Air Systems Command (320) ATTN: Mr. G. L. Desmond Washington, D.C. 20360	1
Commander Naval Air Systems Command (3032) ATTN: Mr. F. W. S. Locke Washington, D.C. 20360	1
Commander Naval Air Systems Command (5301) ATTN: Mr. William Kovin Washington, D.C. 20360	1

DISTRIBUTION LIST (continued)

Addressee	No. of Copies
Commandant U. S. Marine Corps (AX) Headquarters U. S. Marine Corps Washington, D.C. 20025	1
Commandant U. S. Marine Corps (AX-5) Headquarters U. S. Marine Corps ATTN: Col. J. F. Paul Washington, D.C. 20025	1
U. S. Marine Corps Marine Corps Schools (CMCLFDA) Quantico, Virginia 22134	1
Chief of Naval Research Navy Department Air Programs Branch ATTN: Mr. Dean Lauver Washington, D.C. 20325	1
Commanding Officer and Director Naval Ship Research and Development Center Aerodynamics Laboratory (046) Washington, D.C. 20007	1
Director Aeronautical Research National Aeronautics and Space Administration Washington, D.C. 20325	1
National Aeronautics and Space Administration Ames Aeronautical Laboratory Moffett Field, California 94035	1
National Aeronautics and Space Administration Langley Aeronautical Laboratory Langley Field, Virginia 23365	1
National Aeronautics and Space Administration Lewis Flight Propulsion Laboratory Cleveland, Ohio 44118	1
Bell Aerospace Corporation ATTN: Technical Library P. O. Box 1 Buffalo, New York 14200	1

DISTRIBUTION LIST (continued)

Addressee	No. of Copies
The Boeing Company ATTN: Technical Library 7755 East Marginal Way Seattle, Washington 98108	1
Cornell Aeronautical Laboratory, Inc. ATTN: Library 4455 Genessee Street Buffalo, New York 14221	1
Douglas Aircraft Company ATTN: Max Klotzsche C1-23 3855 North Lakewood Boulevard Long Beach, California 90808	1
Douglas Aircraft Company ATTN: Technical Library 3000 Ocean Park Boulevard Santa Monica, California 90405	1
Grumman Aircraft Engineering Corporation ATTN: Library South Oyster Bay Road Bethpage, Long Island, New York 11714	1
Lockheed Aircraft Corporation California Division 2555 North Hollywood Way Burbank, California 91502	1
McDonnell Aircraft Corporation ATTN: Library P. O. Box 516 St. Louis, Missouri 63100	1
North American Aviation, Inc. ATTN: Library International Airport Los Angeles, California 90009	1
Northrop Corporation Norair Division ATTN: Library 1001 East Broadway Hawthorne, California 90250	1

DISTRIBUTION LIST (concluded)

Addressee	No. of Copies
Republic Aviation Corporation ATTN: Library Farmingdale, Long Island, New York 11735	1
United Aircraft Corporation Research Laboratories ATTN: Library 400 Main Street East Hartford, Connecticut 06118	1

UNCLASSIFIED
Security Classification

DOCUMENT CONTROL DATA - R&D

(Security classification of title, body of abstract and indexing annotation must be entered when the overall report is classified)

1. ORIGINATING ACTIVITY (Corporate author) LTV Aerospace Corporation	2a. REPORT SECURITY CLASSIFICATION Unclassified 2b. GROUP

3. REPORT TITLE

Design, Fabrication, Testing, and Data Analysis of ADAM II Concept - Part II

4. DESCRIPTIVE NOTES (Type of report and inclusive dates)

Final Report 2 December 1966 - 7 July 1967

5. AUTHOR(S) (Last name, first name, initial)

Part II - Robert D. Meyer, Robert B. English, Jim K. Davidson

6. REPORT DATE	7a. TOTAL NO. OF PAGES	7b. NO. OF REFS
May 1968		

8a. CONTRACT OR GRANT NO. AF33(615)-3293	9a. ORIGINATOR'S REPORT NUMBER(S)
b. PROJECT NO. 1366	
c. Task No. 136617	9b. OTHER REPORT NO(S) (Any other numbers that may be assigned this report)
d.	AFFDL-TR-68-31, Part II

10. AVAILABILITY/LIMITATION NOTICES This document is subject to special export controls, and each transmittal to foreign governments or foreign nationals may be made only with prior approval of Air Force Flight Dynamics Laboratory (FDMM), Wright-Patterson Air Force Base, Ohio, 45433

11. SUPPLEMENTARY NOTES	12. SPONSORING MILITARY ACTIVITY
All parts are required for a complete understanding of subject	U.S. Air Force Flight Dynamics Lab., Air Force Systems Command, WPAFB, Ohio. U.S. Army Aviation Materials Lab.Ft. Eustis,Va.

13. ABSTRACT

This report contains in four parts, the details of design, fabrication, low and transonic speed wind tunnel testing of a powered propulsive wing model of the LTV ADAM II, V/STOL Aircraft Concept. Part I of this report contains the details of the design and fabrication of the model and includes a description of a new type of "flow-thru" internal strain-gage balance that was developed specifically for testing the model at transonic speeds. Parts II, III, and IV contain analyses of the results from three separate wind tunnel tests. Results presented in these volumes concern the hover, transition, and cruise flight modes. Adequate low speed pitch control power is demonstrated with the use of a vectored thrust nose fan. Cruise mode tests indicate that satisfactory flying qualities can be achieved. A high drag rise Mach number is verified. Requirements for further wind tunnel testing are indicated.

DD FORM 1 JAN 64 1473

UNCLASSIFIED
Security Classification

14. KEY WORDS	LINK A		LINK B		LINK C	
	ROLE	WT	ROLE	WT	ROLE	WT
a. ADAM II, V/STOL Propulsive Wing Aircraft						
b. Powered Model Testing						
c. "Flow-Thru" Balance						
d. High Bypass Ratio Fans						
e. Vectored Thrust						
f. Propulsive Interactions						
g. Sting Interference						
h. Jet Flap						
i. Jet Augmented Flap						
j. Outboard Tails						
k. Delayed Drag Rise						
l. Pitch Control Nose Fan						
m. Ground Effects						
n. Integrated Aerodynamic, Propulsive and Structural Systems						

INSTRUCTIONS

1. ORIGINATING ACTIVITY: Enter the name and address of the contractor, subcontractor, grantee, Department of Defense activity or other organization *(corporate author)* issuing the report.

2*a*. REPORT SECURITY CLASSIFICATION: Enter the overall security classification of the report. Indicate whether "Restricted Data" is included. Marking is to be in accordance with appropriate security regulations.

2*b*. GROUP: Automatic downgrading is specified in DoD Directive 5200.10 and Armed Forces Industrial Manual. Enter the group number. Also, when applicable, show that optional markings have been used for Group 3 and Group 4 as authorized.

3. REPORT TITLE: Enter the complete report title in all capital letters. Titles in all cases should be unclassified. If a meaningful title cannot be selected without classification, show title classification in all capitals in parenthesis immediately following the title.

4. DESCRIPTIVE NOTES: If appropriate, enter the type of report, e.g., interim, progress, summary, annual, or final. Give the inclusive dates when a specific reporting period is covered.

5. AUTHOR(S): Enter the name(s) of author(s) as shown on or in the report. Enter last name, first name, middle initial. If military, show rank and branch of service. The name of the principal author is an absolute minimum requirement.

6. REPORT DATE: Enter the date of the report as day, month, year; or month, year. If more than one date appears on the report, use date of publication.

7*a*. TOTAL NUMBER OF PAGES: The total page count should follow normal pagination procedures, i.e., enter the number of pages containing information.

7*b*. NUMBER OF REFERENCES: Enter the total number of references cited in the report.

8*a*. CONTRACT OR GRANT NUMBER: If appropriate, enter the applicable number of the contract or grant under which the report was written.

8*b*, 8*c*, & 8*d*. PROJECT NUMBER: Enter the appropriate military department identification, such as project number, subproject number, system numbers, task number, etc.

9*a*. ORIGINATOR'S REPORT NUMBER(S): Enter the official report number by which the document will be identified and controlled by the originating activity. This number must be unique to this report.

9*b*. OTHER REPORT NUMBER(S): If the report has been assigned any other report numbers *(either by the originator or by the sponsor)*, also enter this number(s).

10. AVAILABILITY/LIMITATION NOTICES: Enter any limitations on further dissemination of the report, other than those imposed by security classification, using standard statements such as:

(1) "Qualified requesters may obtain copies of this report from DDC."

(2) "Foreign announcement and dissemination of this report by DDC is not authorized."

(3) "U. S. Government agencies may obtain copies of this report directly from DDC. Other qualified DDC users shall request through
____."

(4) "U. S. military agencies may obtain copies of this report directly from DDC. Other qualified users shall request through
____."

(5) "All distribution of this report is controlled. Qualified DDC users shall request through
____."

If the report has been furnished to the Office of Technical Services, Department of Commerce, for sale to the public, indicate this fact and enter the price, if known.

11. SUPPLEMENTARY NOTES: Use for additional explanatory notes.

12. SPONSORING MILITARY ACTIVITY: Enter the name of the departmental project office or laboratory sponsoring *(paying for)* the research and development. Include address.

13. ABSTRACT: Enter an abstract giving a brief and factual summary of the document indicative of the report, even though it may also appear elsewhere in the body of the technical report. If additional space is required, a continuation sheet shall be attached.

It is highly desirable that the abstract of classified reports be unclassified. Each paragraph of the abstract shall end with an indication of the military security classification of the information in the paragraph, represented as *(TS)*, *(S)*, *(C)*, or *(U)*.

There is no limitation on the length of the abstract. However, the suggested length is from 150 to 225 words.

14. KEY WORDS: Key words are technically meaningful terms or short phrases that characterize a report and may be used as index entries for cataloging the report. Key words must be selected so that no security classification is required. Identifiers, such as equipment model designation, trade name, military project code name, geographic location, may be used as key words but will be followed by an indication of technical context. The assignment of links, roles, and weights is optional.